NASA Technical Memorandum 102351

Thermodynamic Properties of Some Metal Oxide-Zirconia Systems

Nathan S. Jacobson
Lewis Research Center
Cleveland, Ohio

December 1989

THERMODYNAMIC PROPERTIES OF SOME METAL OXIDE-ZIRCONIA SYSTEMS

Nathan S. Jacobson
National Aeronautics and Space Administration
Lewis Research Center
Cleveland, Ohio 44135

Summary

Metal oxide-zirconia systems are a potential class of materials for use as structural materials at temperatures above 1900 K. These materials must have no destructive phase changes and low vapor pressures. Both alkaline earth oxide (MgO, CaO, SrO, and BaO)-zirconia and some rare earth oxide (Y_2O_3, Sc_2O_3, La_2O_3, CeO_2, Sm_2O_3, Gd_2O_3, Yb_2O_3, Dy_2O_3, Ho_2O_3, and Er_2O_3)-zirconia systems are examined. For each system, the phase diagram is discussed and the vapor pressure for each vapor specie is calculated via a free energy minimization procedure. The available thermodyamic literature on each system is also surveyed. Some of the systems look promising for high temperature structural materials.

I. Introduction

The developement of engine materials has been dictated by ever increasing demands for high temperature operation. In a recent report[1] on potential materials for engine applications above 3000 F (1900 K), the various issues involved in selection of such a material were outlined. A primary issue at these high temperatures is surface stability, in particular oxidation resistance. At lower temperatures, metals and non-oxides achieve their oxidation resistance by the formation of a protective oxide film. However at temperatures above 1900 K, it was shown that transport rates are so fast that reasonable environmental durability cannot be achieved with a non-oxide. Therefore it was concluded that oxides showed the most promise for application at temperatures above 1900 K.

The criteria for selecting an oxide include a high melting point, low vapor pressure, and solid phase stability. One of the most interesting refractory oxides is ZrO_2, which has a melting point of 2973 K and a low vapor pressure. The primary difficulty with zirconia are its phase changes[2]:

$$\text{Monoclinic} \underset{1223\ K}{\overset{1443\ K}{=}} \text{Tetragonal} \overset{2643\ K}{=} \text{Cubic} \qquad (1)$$

The first phase change is the most catastrophic. In addition zirconia has limited thermal shock resistance.

The solution to the phase change problem has been to add a second oxide[3]. Depending on the amount of second oxide added, this can work in several ways. A small amount can stabilize a mixture of the monoclinic and tetragonal phase. This is known as partially stabilized zirconia and has generated a great deal of interest.[4-6] For the temperatures greater than 1900 K, partially stabilized zirconia is of limited interest. A further addition of a second oxide leads to formation of the cubic phase and is termed fully stabilized zirconia. These systems are of interest in the extremely high temperature range. Finally some oxides form compounds with zirconia. These compounds may show the desirable properties of zirconia and eliminate some of the less desirable properties.

The purpose of this report is to discuss the thermodynamic properties of a number of these systems. The primary emphasis will be on fully stabilized cubic zirconia and high melting zirconia-metal oxide compounds. The requirements for fully stabilized zirconia are not completely understood. The second oxide must be cubic and the metal must be of a comparable ionic radius[3]. For these high temperatures the second oxide must be refractory. There is also some evidence that strong interactions between the

zirconia and the second oxide should not occur. The most common stabilizers are the alkaline earth oxides--MgO and CaO. These systems will be discussed in detail. The remaining alkaline earth oxides--SrO and BaO--do not stabilize the cubic phase, but form high melting compounds with zirconia. These will also be discussed. In addition to the alkaline earth metal oxides, many of the rare earth oxides are stabilizers for zirconia. The systems which will be discussed are CeO_2-ZrO_2, Y_2O_3-ZrO_2, Sc_2O_3-ZrO_2, La_2O_3-ZrO_2, Sm_2O_3-ZrO_2, Gd_2O_3-ZrO_2, Yb_2O_3-ZrO_2, Dy_2O_3-ZrO_2, Ho_2O_3-ZrO_2, and Er_2O_3-ZrO_2. In general these oxide additions do not form compounds with ZrO_2, but they do stabilize the cubic phase.

As mentioned, kinetics for temperatures greater than 1900 K are generally quite rapid. Therefore thermodynamics can be used with good reliability to predict the chemical behavior of a particular material at these temperatures. The major concern is volatility. Vapor pressures for each of the various oxide systems are presented. The best thermodynamic data available is used. The appendix includes a discussion of the sources of thermodynamic data and a complete listing of the data used.

There are a number of issues to be considered in these vapor pressure calculations. Consider first pure $ZrO_2(s)$. It is known to vaporize as follows[7,8]:

$$ZrO_2(s) = ZrO_2(g) \quad (2)$$

$$ZrO_2(s) = ZrO(g) + O(g) \quad (3)$$

$$ZrO_2(s) = Zr(g) + O_2(g) \quad (4)$$

Subject to the mass balance constraint in a closed system:

$$2\ \Sigma\ Zr \text{ containing species in the vapor} = \Sigma\ O \text{ containing species in the vapor} \quad (5)$$

These four equations can be solved simultaneously or a free energy minimization program such as SOLGASMIX[9] can be used. It should be noted that in order to obtain equilibrium vapor pressures from SOLGASMIX, one atomosphere of argon was put in as a reactant. The results of such a calculation for pure ZrO_2 are shown in Figure 1, based on data listed in the appendix. For reactions (3) and (4), where oxygen is released, an overpressure of oxygen will suppress the vaporization process. Figure 2 shows the dramatic effect of one atmosphere of oxygen on suppressing the amount of ZrO(g) and Zr(g). However for reaction (2) where no oxygen is released, the oxygen atmosphere has no effect. Thus it is

important to know the dominant vaporization route in assessing an oxide's performance in a particular high temperature environment.

In many cases, the second oxide may have a much higher vapor pressure than ZrO_2. This vapor pressure can be calculated using the SOLGASMIX program, with the mass balance now including both metal atoms. Corrections for the lowering of the vapor pressure by the particular solid solution must also be considered. Vapor pressures for a number of alkaline earth--zirconia and rare earth--zirconia systems will be presented in this report. The thermodynamic data used for each of these systems is listed in the appendix. It has been pointed out that in some situations the vaporization of binary oxides is complicated by the presence of binary oxides in the vapor, such as $LiBO_2(v)$ over $Li_2O{\cdot}B_2O_3$.[10] In a case like this, the binary oxide cannot be treated as a pseudo-binary system. The vapor pressures of each constituent oxide can no longer be simply calculated from the vapor pressures of the pure oxides and their activities in solution. There is no evidence of this occuring in the various zirconia-metal oxide systems discussed here, but one must be aware of this possibility.

Other factors which can be predicted from thermodynamics include phase changes, reactivity with other gases, and oxide

demixing. As mentioned, the purpose of the second oxide is to eliminate the destructive phase changes present in pure ZrO_2. This can be checked with an accurate phase diagram, which unfortunately is not available for all systems. Reactivity with other gases depends on the application, but is likely to include water vapor.

Oxide demixing is not entirely a thermodynamic problem, but should be considered in any discussion of binary oxides at high temperatures.[11,12] In many applications, such as coatings, the oxide may be under an oxygen potential gradient. Under these conditions, the faster moving metal ion is likely to move to the region of lower oxygen potential. This composition change in the ceramic may lead to a degradation in high temperature properties.

II. Alkaline Earth Oxides-Zirconia Systems

$MgO-ZrO_2$ System

This system has been the subject of numerous studies. Despite these studies, the phase diagram is not firmly established. The most recent phase diagram is shown in

Figure 3.[13] As mentioned, the primary field of interest is the cubic phase field. This phase has a eutectoid at 1679°K (1406°C) and 13.5 mol/o MgO.

Eutectoid decomposition of the cubic phase is a feature of both MgO and CaO stabilized ZrO_2. Clearly this is a factor in cycling cubic ZrO_2:

$$c(ss) \rightarrow t(ss) + MgO \qquad (6)$$

This phase transformation has been studied in detail[14] and is fairly slow. It is also further slowed by the addition of SrO.[14] At still lower temperatures, the tetragonal phase would decompose into the monoclinic phase. Both phase transformations may cause difficulties, particularly the latter.

The liquidus diagram for ZrO_2-MgO is shown in Figure 4.[15] There is a eutectic with the 1:1 mixture at 2100°C, which is agreed on by several investigators.[13,14] However there is some question about the existence of an intermediate compound. Most of the phase diagrams do not show an intermediate compound. However $MgO \cdot ZrO_2$ is available commercially.* Several investigators have reported

*Alfa Products, Danvers, MA.

metastable ordered compounds of composition 2 MgO·5 ZrO_2 and MgO·6 ZrO_2.[13]

One of the major obstacles to the use of this material is the high vapor pressure of MgO--it will preferentially vaporize.[13,16] Vaporization studies of MgO indicate that the primary decomposition products are Mg(g) and O(g), with only a very small amount of MgO(g).[17] We were unable to find data on how activity of MgO changes in solution. In order to estimate an upper limit, we shall use the value of a(MgO) along the MgO-rich cubic phase boundary. Since this is in equilibrium with essentially pure MgO, the activity of MgO is essentially unity. Based on this, the vapor pressure for MgO is shown in Figure 5.

CaO-ZrO_2 System

This system is similar to the MgO-ZrO_2 system, but has some important differences. A recent phase diagram is shown in Figure 6.[18] Unlike the MgO-ZrO_2 system, there is general agreement on the formation of several stable intermediate compounds. At lower temperatures, there is a compound CaO·4(ZrO_2). There is also a compound CaO·ZrO_2, which is stable to its melting point of 2252 K. This compound itself has been considered for use as an ultra high temperature structural material and will be discussed. Like the

$MgO-ZrO_2$ system, the $CaO-ZrO_2$ system forms cubic phase euctectoid and its decomposition must be considered.

The $CaO-ZrO_2$ system is quite suitable for electrochemical measurements and there is some information on the activity of CaO in solid ZrO_2 solution.[19,20] These measurements use a cell of the form:

$$O_2,Pt|CaO,CaF_2|CaF_2|ZrO_2\text{-}CaO,CaF_2|Pt,O_2 \qquad (7)$$

The overall cell reaction is simply:

$$CaO(a=1) = CaO(\text{solid solution}) \qquad (8)$$

$$\Delta G = -2EF = -RT \ln a(CaO\text{-}ss) \qquad (9)$$

Here ΔG is the Gibbs free energy of formation, E is the measured EMF, F is the Faraday constant, and R is the gas constant. Measurements are carried out between 1200 and 1550 K and the results are shown in Figure 7. These temperatures are somewhat lower than those of interest to us, but nonetheless, the measurements give an indication of the strong negative deviations from Raoult's Law, as shown in the diagram. These indicate a strong interaction between CaO and ZrO_2 which is not surprising, given the eventual compound formation. Note the CaO activity is about an order of

magnitude lower than that predicated for Raoult's law behavior or in total about two orders of magnitude lower than for pure CaO. This type of data is very important in evaluating the suitablity of ZrO_2 cubic solid solutions for use at very high temperatures.

These data also point to the as-yet unsettled differences in the CaO-ZrO_2 phase diagram. They suggest a a temperature independent solubility limit of 17 m/o CaO in ZrO_2 over the temperature range 1200-1500 K. The most recent phase diagram (Figure 6) shows a solubility limit of about 7 m/o CaO below 1413 K and a temperature dependent solubility limit which is about 17 m/o CaO at 1413 K and above. These differences are very likely due to the slow phase changes at these temperatures.

Vapor pressure calculations for both pure CaO and $CaZrO_3$ are shown in Figures 8 and 9. For CaO, as with MgO, the primary vapor products are the metal atom and oxygen. These figures indicate the compound lowers the vapor pressure of Ca by about two orders of magnitude. This is consistant with the solid solution data in Figure 7, for the solid solution in equilibrium with the compound.

SrO-ZrO_2

This system and the BaO-ZrO_2 system differ from the two systems previously discussed in that there is limited solid solubility and the cubic phase is not stabilized. The reasons for this are not entirely clear. Some authors have given arguments based on size factors[3]--the strontium and barium atoms have radii too large to enter the zirconia lattice. Other authors have based arguments on thermodynamic factors[20]--the strontium and barium zirconates are so stable that a two phase region of zirconia and zirconate is favorable over a solid solution.

Therefore in this system, the materials of interest are the compounds. These are shown in the phase diagram[21] in Figure 10. There are several high melting intermediate phases, including $SrZrO_3$, $Sr_4Zr_3O_{10}$, and Sr_2ZrO_4. The first of these has a low coefficient of thermal expansion, suggesting good resistance to thermal shock.[1]

The calculated vapor pressures for the vapor above SrO and $SrZrO_3$ are shown in Figures 11 and 12. As with the other systems discussed, the alkaline earth oxide vaporizes preferentially to the metal atom and atomic and molecular oxygen, with the metal oxide vapor roughly an order of magnitude lower.

It has been reported that this material is quite susceptible to oxide demixing, with a strong separation appearing between the SrO and ZrO_2 oxides under the influence of an oxygen potential.[22] This behavior must be considered when using this material under such conditions. Although not shown on the phase diagram, it has also been reported that $SrZrO_3$ undergoes the following phase transformations[23]:

$$\text{orthorhombic} \xrightarrow{923\ K} \text{tetragonal 1} \xrightarrow{1003\ K} \text{tetragonal 2} \xrightarrow{1443\ K} \text{cubic} \quad (10)$$

These may be limiting factors in the application of $SrZrO_3$ as a structural material.

BaO-ZrO_2

This system is somewhat similar to the SrO-ZrO_2 system in that BaO does not stablize cubic ZrO_2. We could not locate a phase diagram for this binary system. However $BaZrO_3$ is known to be a stable compound and there are several sources of thermodynamic data for the solid as well as vapor pressure measurements.

Figures 13 and 14 show the vapor pressures for the major vapor species over BaO and $BaZrO_3$. Note that the major vapor specie is BaO(g), not the metal atoms and oxygen as in the other systems discussed. This is important, since an oxygen overpressure will not suppress vaporization in this case.

Figure 15 shows the experimental data[10,24-27] on $BaZrO_3$. Note the calculated vapor pressures from the thermdynamic data in the appendix is somewhat lower than the measured P(BaO). It may be that the measured $BaZrO_3$ compounds are a little BaO rich or there may be some inconsistancies in the thermodynamic data. The Odoj and Hilpert[24-26] data was taken with a Knudsen Cell Mass Spectrometer using a molybdenum cell. There was no evidence of reaction with the cell. The data of Berkowitz-Mattuck[10] was taken with a Knudsen Cell Mass Spectrometer and a rhenium cell. The rhenium cell is expected to be more inert than the molybdenum cell. The data of Glenn et. al.[27] is an <u>not</u> equilibrium measurement--it was simply the recession rate of an exposed surface. This was converted to a vapor pressure by the Hertz-KnudsenLangmuir equation:

$$J=P/(2\pi MRT)^{1/2} \qquad (11)$$

Here J is the flux leaving the surface, P is the vapor pressure, M is the molecular weight of the vapor leaving the surface, R is the gas constant, and T is the temperature. When the appropriate conversion factors are added, this equation becomes:

$$P(atm)=(2.26\times10^{-2})J(mole/cm^2\text{-}sec)(M(gm/mole))^{1/2}(T(^{o}K))^{1/2} \qquad (12)$$

Despite the fact that this is a non-equilibrium measurement, the pressures measured are quite close to the calculated

equilibrium values.

In general the alkaline-stabilized zirconia cubic solutions compounds have some severe limitations for applications above 1900 K. The major problem is likely to be preferential volatilization of the alkaline earth oxides. Other difficulties include phase changes and possible oxide demixing. The materials with the least limitations are $SrZrO_3$ and $CaZrO_3$.

III. Rare Earth Oxide-Zirconia Systems

The rare earth oxide-zirconia systems may be more promising. In general they have lower vapor pressures and some exhibit very high melting points. The Russian group of Belov and Semenov[28-32] have looked extensively at these binary oxide systems.

Consider first the the pure rare earth oxides. These vaporize as follows:

$$M_2O_3(s) = 2\ MO(g) + O(g) \qquad (13)$$

This is with the exception of Yb, which decomposes as:

$$Yb_2O_3(s) = 2\ Yb(g) + 3\ O(g) \qquad (14)$$

In their initial survey, Belov and Semenov[28] list the various rare earth oxides and their vapor pressures relative to Lu_2O_3. Their data is given in Table I. They also point out that the zirconia systems with Gd_2O_3, Dy_2O_3, Yb_2O_3, Ho_2O_3, Er_2O_3, and Y_2O_3 exhibit liquidus maxima. They studied the volatilization of each of these and the Lu_2O_3-ZrO_2 system in the temperature range 2773-2823 K. Only the Yb_2O_3-ZrO_2 and Gd_2O_3-ZrO_2 systems decompose, preferentially losing the stabilizing oxide.

Belov and Semenov have examined a range of rare earth oxide-zirconia stabilized systems and found the following general behavior. These systems first undergo a period of incongruent vaporization, during which the oxides loose oxygen and go from $ZrO_2(M_2O_3)$ to $ZrO_{2-x}(M_2O_{3-y})$. The oxygen pressure created tends to suppress decomposition vaporization reactions, such as 3, 4, 13 and 14. After this a period of congruent vaporization begins.

The activities of the two oxide components can be determined from the congruent vaporization stage. Typically the activity of a component in solution is given by:

$$a(i) = P(i)/P^{o}(i) \qquad (15)$$

Here P(i) is the vapor pressure of the component in solution

and $P^{o}(i)$ is the vapor pressure of the pure component. In the case of a rare-earth oxide-zirconia system, the activity of zirconia can be calculated as:

$$a(ZrO_2) = P(ZrO_2)/P^{o}(ZrO_2) \qquad (16)$$

However the mass spectrometer intensity of the ZrO_2^+ ion may not always be easy to determine as a function of composition. Therefore it is desirable to use the other ions to determine activities of the components.

Belov[32] points out that use of the other ions is more complex because they are dissociation products. He proposes a calculation method based on the intensity of the MO^+ ion from M_2O_3, as a function of composition. The two primary vaporization routes for ZrO_2 and M_2O_3 are given by equations (3) and (13). The equilibrium constants give the following relations:

$$a(ZrO_2) = P(ZrO)\ P(O\text{-tot}) \ /\ P^{o}(ZrO)\ P^{o}(O\text{-tot}) \qquad (17)$$

$$a(M_2O_3) = P(MO)^2\ P(O\text{-tot}) \ /\ P^{o}(MO)^2\ P^{o}(O\text{-tot}) \qquad (18)$$

Note that P(O-tot) is the amount of O from both ZrO_2 decomposition, $P(O\text{-}ZrO_2)$, and M_2O_3 decomposition, $P(O\text{-}M_2O_3)$. The actual calculation is iterative. The first step involves

setting P(ZrO) = O and taking P(O-tot) = P(O-M_2O_3). This is in equation (18) to calculate the value of a(M_2O_3). Then the Gibbs-Duhem equation is used to calculate a(ZrO_2). This value is put into equation (17) to calculate P(ZrO) and P(O-ZrO_2). The new P(O-tot) becomes P(O-M_2O_3) + P(O-ZrO_2) and the second iteration begins. This continues until the iterations converge. This is an important and useful technique for obtaining activities in these complex oxide systems.

In the following discussion of rare earth oxide-zirconia stabilized materials, a number of sytems will be discussed. Their vapor pressures and solid solution behavior will be discussed.

Y_2O_3-ZrO_2

This is the most common of the rare earth stabilized zirconia systems. A recent phase diagram[33] is shown in Figure 16. Note that the cubic phase field does not extend to lower temperatures, but undergoes a eutectoid decomposition, similar to that of the MgO and CaO stabilized zirconia. This phase change is slow and has only been recently detected.

Figure 17 is an activity-composition diagram determined by mass spectrometry[30] for this system. This data was

obtained by the two calculation methods described in the preceeding discussion. Note the negative deviations from Raoult's Law, indicating attractive interactions. However interactions are stronger in the $CaO-ZrO_2$ system (Figure 7), in which compound formation is eventually observed.

Figures 18 shows the calculated vapor pressures above pure Y_2O_3 as well as some data points for the vapor pressure of $YO(g)$[34] above Y_2O_3. These show good agreement with the calculated values. Figure 19 shows the calculated vapor pressures above $Y_2O_3 \cdot 2(ZrO_2)$. Note that the vapor pressures of YO(g) and Y(g) are lowered by less then an order of magnitude, which is consistant with Figure 17.

Some recent evidence[35] indicates that the Y_2O_3 in this material reacts with water. This is an important point which merits further investigation for structural applications of this material.

$Sc_2O_3-ZrO_2$

This system is of interest due the low density of Sc_2O_3. Figure 20 shows a phase diagram[36]. There are some low temperature phase changes and the location of the liquidus is still in question. However there is a large cubic phase field.

Semenov[37] and Belov et. al.[38-39] have investigated the vaporization behavior of pure Sc_2O_3 and Sc_2O_3-ZrO_2 solid solutions. For the solid solutions, they observe the following near ideal behavior:

$$P(ScO\text{-}sol)=P^{o}(ScO)[x(Sc_2O_3)] \qquad (15)$$

From this relation and the iterative calculation method described above, they calculate an activity-composition diagram is shown in Figure 21. Note the similarity to that for Y_2O_3-ZrO_2. Both exhibit negative deviations from Raoult's Law, indicating attractive forces.

Figure 22 is a plot of the calculated vapor pressures above pure Sc_2O_3 and the experimental data of Semenov[37], which is in good agreement. In the Sc_2O_3-ZrO_2 solution, one would expect limited vapor pressure lowering consistent with Figure 21 and similar to the $Y_2O_3 \cdot 2(ZrO_2)$ case. It should be noted that the vapor pressure in the solid solution is sufficiently high that Belov et. al.[38] observe after 100 minutes at 2580^{o}K, all the Sc_2O_3 has vaporized from their sample of 50 m/o Sc_2O_3 - 50 m/o ZrO_2.

La_2O_3-ZrO_2

The phase diagram for this system[40] is shown in Figure 23. While the cubic phase undergoes a eutectoid decomposition at about 2248 K, there is a pyrochlore phase which seems to be stable over a wide range of temperatures.

Figures 24 and 25 show the vapor pressure above La_2O_3 and $La_2O_3 \cdot 2(ZrO_2)$, respectively. La_2O_3 has one of the higher vapor pressures of the rare earth oxides (Table I), which would be a limitation of applications of this system. Consistent with the other systems, relatively little vapor pressure lowering is expected in the solid solution (Figure 25).

It is well known that La_2O_3 is quite hygroscopic. This may be also be a limitation in the application of the solid solution.

CeO_2-ZrO_2

There is currently interest in the partially stabilized zirconia of this system.[41] However, as shown in the phase diagram (Figure 26), there is not a fully stabilized composition down to low temperatures for this system. The catastrophic monoclinic to tetragonal phase transformation

limits this material's use as a high temperature structural material.

Vapor pressure calculations for pure Ce_2O_3 and $Ce_2Zr_2O_{7-x}$ are shown in Figures 27 and 28. This system also has a rather high vapor pressure, which also limits its application. Note that in Figure 28, the vapor pressure of ZrO and Zr is actually higher than their vapor pressure above pure ZrO_2. This is an interesting consequence of vaporization of Ce_2O_3 as $CeO_2(g)$ and CeO(g). In the solid solution, $Ce_2O_3 \cdot 2(ZrO_2)$, when both these species are formed, very little O(g) is generated. In fact, since the species are not formed in equal amounts, some oxygen must come from ZrO_2. There is no suppression of the vaporization/ decomposition processes (i.e. reactions (3) and (4)) and the vapor pressures of ZrO and Zr go up. These vapor pressures are not simply related to the activity of ZrO_2, which must remain one or less in solution.

Sm_2O_3-ZrO_2 and Gd_2O_3-ZrO_2

The phase diagrams for these two systems appear similar. The phase diagram for the Sm_2O_3-ZrO_2 system[42] is shown in Figure 29. There is a large cubic phase field and also a miscibility gap and temperatures less than 2000 K.

The vapor pressures for Sm_2O_3 are shown in Figure 30. The heat of formation of the solid solution $Sm_2O_3 \cdot 2(ZrO_2)$ has been measured[42]. However, when put into the free energy minimization program, it was found that the solid solution decomposed to the constituent oxides at about 1500 K. This indicates either an inconsistency in the data or the phase diagram. Nonetheless Sm_2O_3 does have a fairly low vapor pressure and stabilizes the cubic phase of ZrO_2.

The phase diagram for the Gd_2O_3-ZrO_2 system[44] is shown in Figure 31. Note the large cubic phase field. The vapor pressures for above pure Gd_2O_3 are shown in Figure 32. The same situation for the free energy minimization as in $Sm_2O_3 \cdot 2(ZrO_2)$ was found, also indicating an inconsistency in the data or the phase diagram. Although Gd_2O_3 is one of the lower vapor pressure rare earth oxides, Belov and Semenov[28] have found that on heating in the range 2773-2823 K, Gd_2O_3 completely vaporizes from a solid solution with ZrO_2.

Yb_2O_3-ZrO_2, Dy_2O_3-ZrO_2, Ho_2O_3-ZrO_2, and Er_2O_3-ZrO_2

These systems all show similar phase diagrams, which exhibit large cubic phase fields and liquidus maxima. These diagrams[45-48] are shown in Figures 33, 35, 37, and 39. Note that in each case the liquidus maxima is at a composition of

0.15 to 0.20 M_2O_3-ZrO_2 and a temperature near 2800 K. The phase diagrams are very likely all somewhat tentative, but they do show a lack of phase changes for these compositions.

As mentioned previously, Yb_2O_3 is one of the few rare earth oxides which decomposes to the metal and oxgyen. Its vapor pressure is shown in Figure 34. Data for the solid oxide solution was not available. Belov and Semenov[28] have noted that in the temperature range 2773 K to 2823 K, Yb_2O_3 tends to completely vaporize from the solid solution.

The vapor pressures above Dy_2O_3, Ho_2O_3, and Er_2O_3 are shown in Figures 36, 38, and 40. Solid solution data was not available. However systems which exhibit liquidus maxima show significant interactions[49] and hence these systems should show a corresponding vapor pressure lowering. Belov and Semenov[28] have shown that each of these systems at 2, 3, 10, and 50 m/o do not decompose at temperatures of 2773-2823 K. They have have also suggested the Lu_2O_3-ZrO_2 system, since Lu_2O_3 has the lowest vapor pressure of the rare earth oxides, as shown in Table I. However a phase diagram could not be located for the Lu_2O_3-ZrO_2 system. Clearly more work is needed on these important systems.

V. Conclusions

The thermodynamic properties of a number of oxide-zirconia systems have been examined. Particular emphasis has been on phase changes and volatility.

The alkaline earth oxide systems have been examined. Magnesia and calcia stabilize zirconia, strontia and baria do not stabilize zirconia but form compounds. Clearly the $MgO-ZrO_2$ and $BaO-ZrO_2$ systems show too much volatility to be useful. The $CaO-ZrO_2$ and $SrO-ZrO_2$ systems may show some limited application.

The rare earth oxide-zirconia systems generally have lower vapor pressures. The $Y_2O_3-ZrO_2$, $Sc_2O_3-ZrO_2$, $La_2O_3-ZrO_2$, $Ce_2O_3-ZrO_2$, $Sm_2O_3-ZrO_2$, $Gd_2O_3-ZrO_2$, $Dy_2O_3-ZrO_2$, $Ho_2O_3-ZrO_2$, and $Er_2O_3-ZrO_2$ systems were examined. The $La_2O_3-ZrO_2$ system has a high vapor pressure and is hygroscopic. The $Ce_2O_3-ZrO_2$ system has a very high vapor pressure and does not really have a fully stabilized cubic structure to lower temperatures. The $Sm_2O_3-ZrO_2$ and $Gd_2O_3-ZrO_2$ system may have some phase changes--more work needs to be done. Previous investigations have suggested that the $Sc_2O_3-ZrO_2$, $Yb_2O_3-ZrO_2$, and $Gd_2O_3-ZrO_2$ systems may have a volatility problem--more work in the temperature range of interest is needed. The $Y_2O_3-ZrO_2$, $Dy_2O_3-ZrO_2$, $Ho_2O_3-ZrO_2$, and $Er_2O_3-ZrO_2$ systems all look quite promising.

They have low vapor pressures and current evidence suggests no serious phase changes. Other more exotic rare earth systems may also show promise.

The purpose of this review has been to bring together all the available thermodynamic data on some metal oxide-zirconia systems. A good deal of this data is from obscure and difficult to locate sources. From this data a number of systems appear promising for use as structural materials in the temperatures above 1900 K. However this review also points towards the need for more data--in particular more phase change information, further vapor pressure measurements, and in general upper temperature limits for the application of each material.

Acknowledgement

Special thanks are due to Dr. Ajay Misra for his assistance in the use of the SOLGASMIX computer program.

Table I. Relative vapor pressures of some rare earth oxides, according to Belov and Semenov[28]

Oxide	Evaporation Rate at 2500 K $W(M_2O_3)/W(Lu_2O_3)$
La_2O_3	130
Nd_2O_3	70
Sm_2O_3	40
Gd_2O_3	15
Dy_2O_3	10
Yb_2O_3	10
Tm_2O_3	6
Ho_2O_3	4
Er_2O_3	4
Y_2O_3	2
Lu_2O_3	1

REFERENCES

1. Shaw, N.J. et. al.: Materials for Engine Applications Above 3000°F - an Overview. NASA TM 100169, 1987.

2. Yoshimura, M.: Phase Stability of Zirconia. Am. Ceram. Soc. Bull., vol. 67, no. 12, 1988, pp. 1950-1955.

3. Ryshkewitch, E. and Richerson, D.W.: Oxide Ceramics. Second Edition, General Ceramics, Inc., Haskell, NJ, 1985, pp. 350-396.

4. Stevens, R.: Zirconia and Zirconia Ceramics. Second Edition, Magnesium Elektron, Ltd., Manchester, U.K., 1986.

5. Nettleship, I. and Stevens, R.: Tetragonal Zirconia Polycrystal (TZP) - A Review. Int. J. High Technol. Ceram., vol. 3, no. 1, 1987, pp. 1-32.

6. Heuer, A.H.: Alloy Design in Partially Stabilized Zirconia. Science and Technology of Zirconia (Advances in Ceramics, Vol. 3), A.H. Heuer and L.W. Hobbs, eds., American Ceramic Society, Columbus, OH, 1981, pp. 98-115.

7. Chupka, W.A.; Berkowitz, J.; and Inghram, M.G.: Thermodynamics of the Zr-ZrO_2 System: The Dissociation Energies of ZrO and ZrO_2. J. Chem. Phys., vol. 26, no. 5, May 1957, pp. 1207-1210.

8. Ackermann, R.J.; and Thorn, R.J.: Vaporization of Oxides. Progress in Ceramic Science, Vol. 1, J.E. Burke, ed., 1961, pp. 39-88.

9. Bessman, T.M.: SOLGASMIX-PV, A Computer Program to Calculate Equilibrium Relationships in Complex Chemical Systems. ORNL/TM-5775, Apr. 1977.

10. Brett, J. et. al.: Experimental Study of Factors Controlling the Effectiveness of High-Temperature Protective Coatings for Tungsten. AFML-TR-64-392, Wright Patterson Air Force Base, Dayton, Ohio, 1965, (Avail. NTIS, AD-619867).

11. Schmalzried, H.; Laqua, W.; and Lin, P.L.: Crystalline Oxide Solid Solutions in Oxygen Potential Gradients. Z. Naturforsch, vol. 34a, no. 2, 1979, pp.192-199.

12. Ishikawa, T., et. al.: Demixing of Materials Under Chemical Potential Gradients. J. Am. Ceram. Soc., vol. 68, no. 1, Jan. 1985, pp. 1-6.

13. Sim, S.M.; and Stubican, V.S.: Phase Relations and Ordering in the System ZrO_2-MgO. J. Am. Ceram. Soc., vol. 70, no. 7, July 1987, pp. 521-526.

14. Farmer, S.R.; Heuer, A.H.; and Hannink, R.H.J.: Eutectoid Decomposition of MgO-Partially-Stabilized ZrO_2. J. Am. Ceram. Soc., vol 70, no. 6, June 1987, pp. 431-440.

15. Noguchi, T.; and Mizuno, M.: Liquidus Curve Measurements in the ZrO_2-MgO System with the Solar Furnace. Bull. Chem. Soc. Japan., vol. 41, no. 7, 1968, pp. 1583-1587.

16. Sakka, Y.; Oishi, Y.; and Ando, K.: Enhancement of MgO Evaporation from MgO-Stabilized ZrO_2 by Grain-Boundary Diffusion. J. Am. Ceram. Soc., vol. 69, no. 2, Feb. 1986, pp. 111-113.

17. Altman, R.A.: Vaporization of Magnesium Oxide and its Reaction with Alumina. J. Phys. Chem., vol. 67, no. 2, Feb. 1963, pp. 366-369.

18. Stubican, V.S.; and Hellman, J.R.: Phase Equilibria in Some Zirconia Systems. Science and Technology of Zirconia

(Advances in Ceramics, vol. 3), A.H. Heuer and L.W. Hobbs, eds., American Ceramic Society, Columbus, OH, 1981, pp. 25-36.

19. Pizzini, S. and Morlotti, R.: E.M.F. Measurements with Solid Electrolyte Galvanic Cells on the Calcium Oxide+Zirconia System. J. Chem. Soc. Faraday Trans. I, vol. 68, 1972, pp. 1601-1610.

20. Levitskii, V.A. et. al.: Thermodynamic Study of Some Solid Solutions in the $CaO-ZrO_2$ System by the emf Method. J. Solid State Chem., vol. 20, no. 2, Feb. 1977, pp. 119-125.

21. Noguchi, T.; Okubo, T.; and Yonemochi, O.: Reactions in the System ZrO_2-SrO. J. Amer. Ceram. Soc., vol. 52, no. 4, Apr. 1969, pp. 178-181.

22. Program Review, Ultra-High Temperature Composite Materials, November 16-17, 1988, Materials Laboratory - Wright Patterson Air Force Base, Dayton, OH.

23. Carlsson, L.: High Temperature Phase Transitions in $SrZrO_3$. Acta. Cryst., vol. 23, pt. 6, Dec. 1967, pp. 901-905.

24. Odoj, R.; and Hilpert, K.: Mass Spectrometric High Temperature Measurements of the Barium Oxide - Zirconium Dioxide System and the Determination of Thermodynamic Data for Barium Zirconate. Clarification of the Counter Stopping Capacity of Coated Particles for Solid Fission Products by Zirconium Dioxide Addition. (Massenspektrometrische Hochtemperature Messung des Systems $BaO-ZrO_2$ and Bestimmung Thermodynamischer Daten des $BaZrO_3$. Ber. Kernforschungsanlage Juelich, 1975) NASA TT-20187, 1988.

25. Odoj, R.; and Hilpert, K.; Evaporation and Standard Enthalpy of Formation of $BaZrO_3(s)$. Z. Phys. Chem. Weisbaden, vol. 102, no. 5-6, Oct. 1976, pp. 191-201.

26. Odoj, R. et. al.: Study of the Retention of Ba in UO_2 Nuclear Fuel Particles by ZrO_2 as Getter. J. Nucl. Mater. vol. 60, no. 2, May 1976, pp. 216-222.

27. Glenn, M.L.; Henry, J.L.; and Adams, A.; Evaluation of Selected Spinels and Perovskites as Candidate High-Temperature Molybdenum Coatings. US Dept. of the Interior, Bureau of Mines BM-RI-8351, 1979.

28. Belov, A.N.; and Semenov, G.A.: Mass-Spectrometric Investigation of Stabilizing Oxides from Solid Solutions

ZrO_2-M_2O_3. Inorg. Mater. (Engl. Transl.), vol. 16, no. 12, Dec. 1980, pp. 1513-1517.

29. Belov, A.N.; Lopatin, S.I.; and Semenov, G.A.: Mass Spectrometric Study of the Incongruent Step in the Evaporation of Lu_2O_3 and of ZrO_2-Y_2O_3 and ZrO_2-Lu_2O_3 Solid Solutions, Russ. J. Phys. Chem., vol. 55, no. 4, Apr. 1981, pp. 524-528.

30. Belov, A.N.; and Semenov, G.A.: Thermodynamics of Binary Solid Solutions of Zirconium, Hafnium, and Yttrium Oxides from High-temperature Mass Spectrometry Data. Russ. J. Phys. Chem., vol. 59, no. 3, Mar. 1985, pp. 342-344.

31. Belov, A.N.; and Semenov, G.A.: Calculation of the Thermodynamic Properties of Binary $ZrO_2(HfO_2)$ - Rare-Earth Element Oxide Solid Solutions from the Volatility of the Indivual Oxides. Russ. J. Phys. Chem., vol. 59, no. 9, Sept. 1985, pp. 1390-1392.

32. Belov, A.N.: Thermodynamics of Binary Solutions with a Common Dissociation Product of the Components in the Gas Phase. Russ. J. Phys. Chem., vol. 59, no. 10, Oct. 1985, pp. 1449-1450.

33. Stubican, V.S.; Hink, R.C.; and Ray, S.P.: Phase Equilibria and Ordering in the System ZrO_2-Y_2O_3. J. Am. Ceram. Soc., vol. 61, no. 1-2, Jan.-Feb. 1978, pp. 17-21.

34. Walsh, P.N.; Goldstein, H.W.; and White, D.: Vaporization of Rare-Earth Oxides. J. Am. Ceram. Soc. vol. 43, no. 5, May 1960, pp. 229-233.

35. Winnubst, A.J.A.; and Burggraaf, A.J.: The Aging Behavior of Ultrafine-Grained Yttria-Containing Tetragonal Zirconia (Y-TZP) in Hot Water. Science and Technology of Zirconia III (Advances in Ceramics, Vol. 24), The American Ceramic Society, Columbus, OH, 1988, pp. 39-47.

36. Levin, E.M.; and McMurdie, H.F., eds.: Phase Diagrams for Ceramists 1975 Supplement. The American Ceramic Society, Columbus, OH, 1975, p. 159.

37. Semenov, G.A.: Mass Spectrometric Investigation of the Vaporization of Scandium Oxide. Russ. J. Inorg. Chem., vol. 10, no. 10, Oct. 1965, pp, 1300-1301.

38. Belov, A.N. et. al.: Evaporation and Thermodynamic Properties of Sc_2O_3 and of ZrO_2-Sc_2O_3 Binary Solid Solutions

According to High-Temperature Mass Spectrometry Data. I. Experimental. Russ. J. Phys. Chem., vol. 61, no. 4, Apr. 1987, pp. 464-468.

39. Belov, A.N. et. al.: Evaporation and Thermodynamic Properties of Sc_2O_3 and of ZrO_2-Sc_2O_3 Binary Solid Solutions According to High-Temperature Mass Spectrometry Data. II. Calculations. Russ. J. Phys. Chem., vol. 61, no. 4, Apr. 1987, pp. 468-470.

40. Roth, R.S.; Negas, T.; and Cook, L.P.: Phase Diagrams for Ceramists Vol. IV. The American Ceramic Society, Columbus, OH, 1981, p. 133.

41. Muroi, T.; Echigoya, J.I.; and Suto, H.: Structure and Phase Diagram of ZrO_2-CeO_2 Ceramics. Trans. Jpn. Inst. Met., vol. 29, no. 8, Aug. 1988, pp. 634-641.

42. op. cit. Reference 40, p. 139.

43. Korneev, V.R.; Glushkova, V.B.; and Keler, E.K.: Heats of Formation of Rare Earth Zirconates. Inorg. Mater. (Engl. Transl.), vol. 7, no. 5, May 1971, pp. 781-782.

44. op. cit. Reference 40, p. 129.

45. op. cit. Reference 40, p. 143.

46. op. cit. Reference 40, p. 125.

47. op. cit. Reference 40, p. 131.

48. op. cit. Reference 40, p. 127.

49. Swalin, R.A.: Thermodynamics of Solids. Second Edition, J. Wiley and Sons, New York, 1972, p. 215.

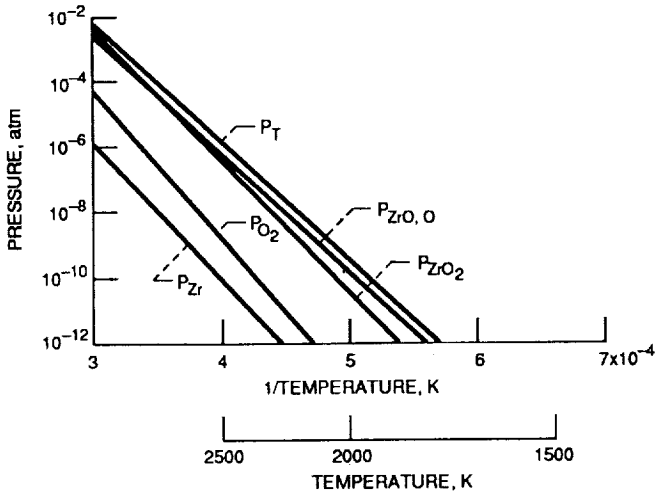

Figure 1. - Vapor pressures above ZrO_2.

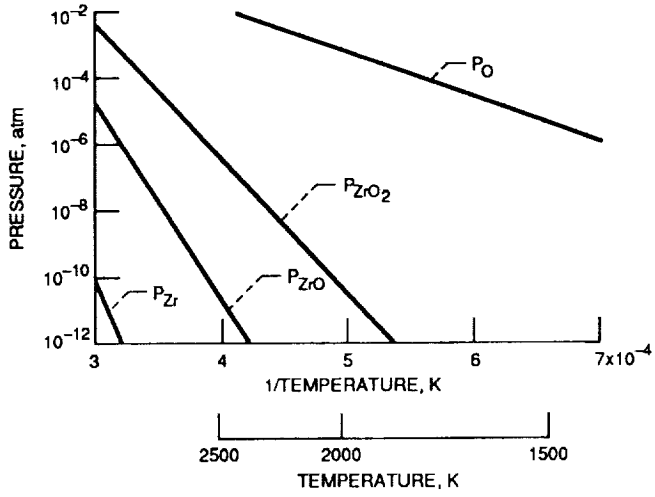

Figure 2. - Vapor pressures above ZrO_2 + 1 atm. O_2.

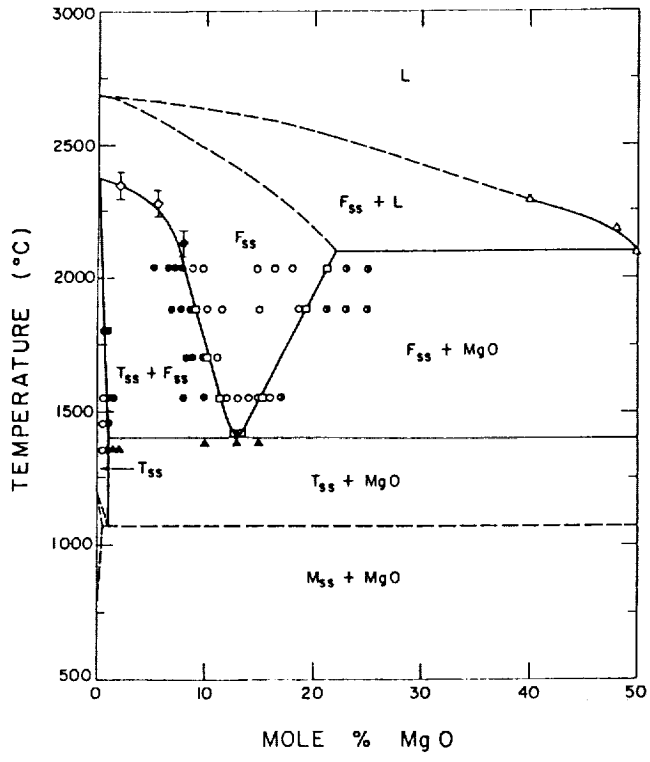

Figure 3. - ZrO_2-MgO phase diagram.[13] Reprinted by permission of the American Ceramic Society.

MgO–ZrO_2

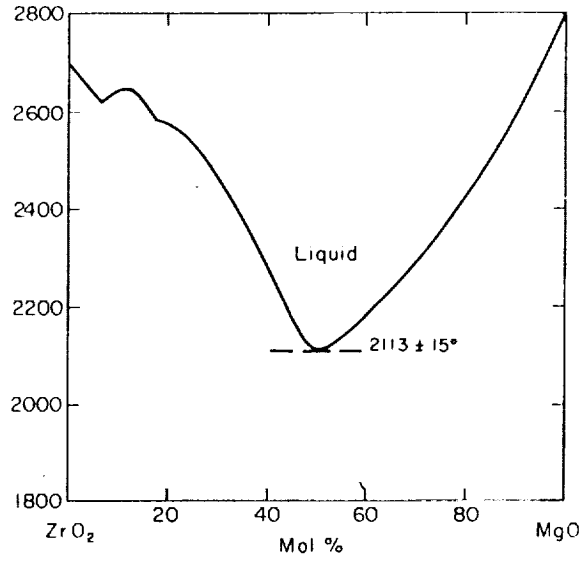

Figure 4. - ZrO_2-MgO liquidus curve.[15,36] Reprinted by permission of the American Ceramic Society.

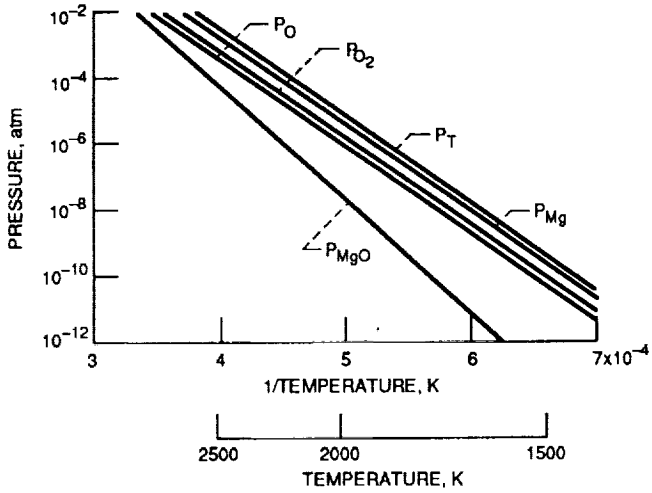

Figure 5. - Vapor pressures above MgO.

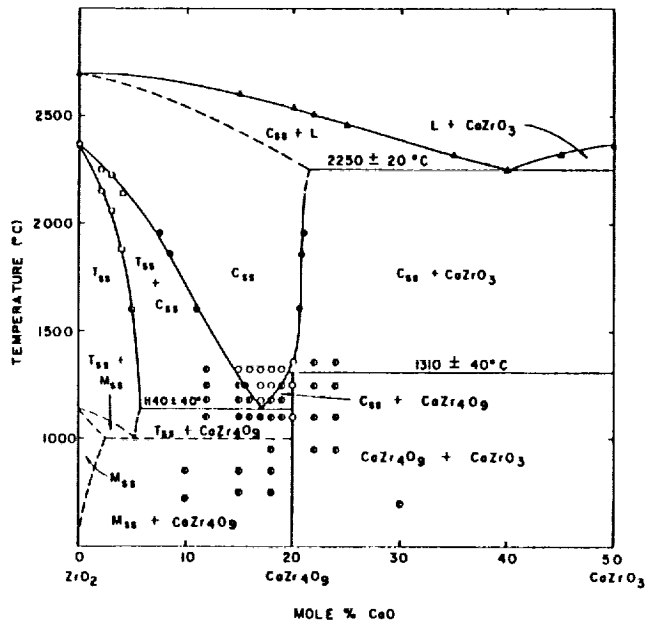

Figure 6. - ZrO_2-CaO phase diagram.[18] Reprinted by permission of the American Ceramic Society.

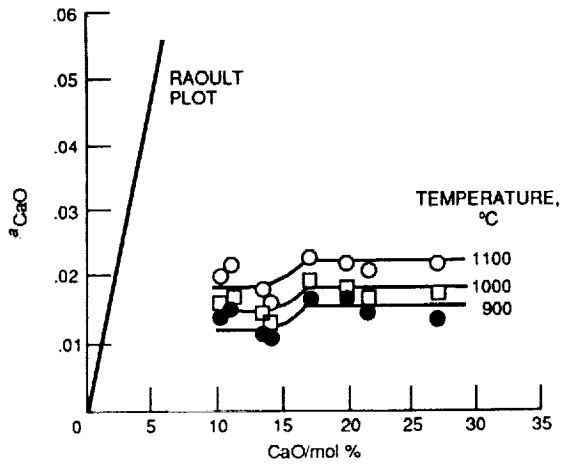

Figure 7. - Activity-Composition diagram for ZrO_2-CaO.[19] Reprinted by permission of the Royal Society of Chemistry.

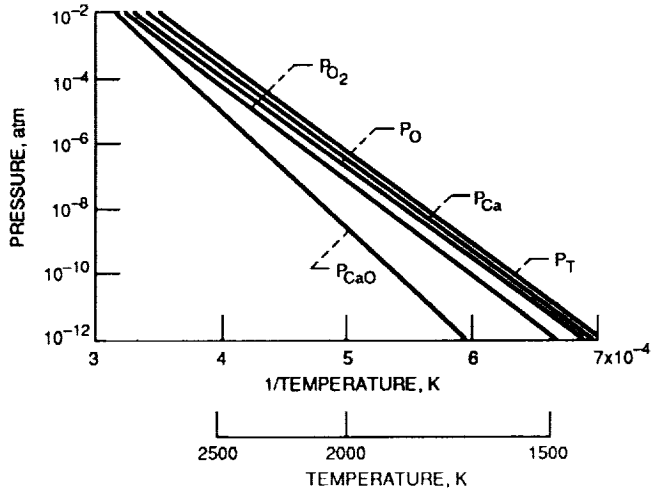

Figure 8. - Vapor pressures above CaO.

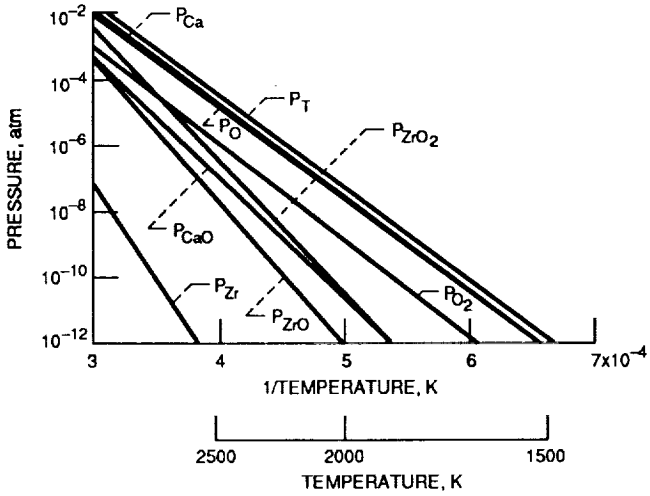

Figure 9. - Vapor pressures above $CaZrO_3$.

$SrO–ZrO_2$

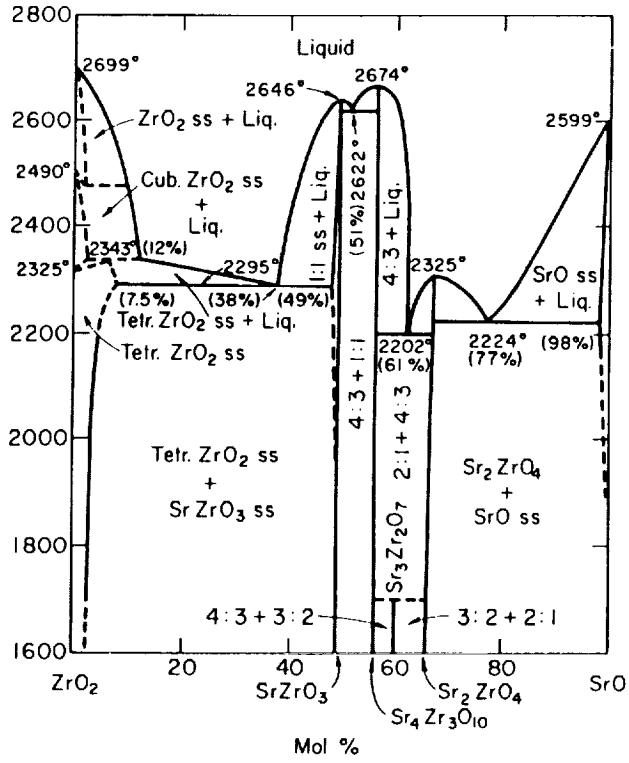

Figure 10. - Phase diagram for ZrO_2-SrO.[21] Reprinted by permission of the American Ceramic Society.

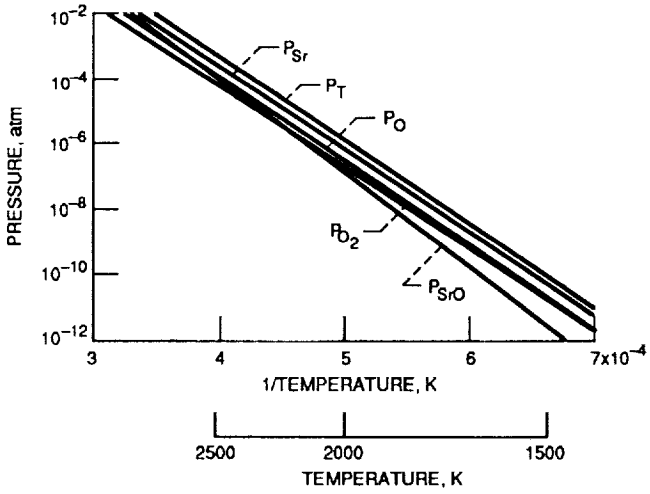

Figure 11. - Vapor pressures above SrO.

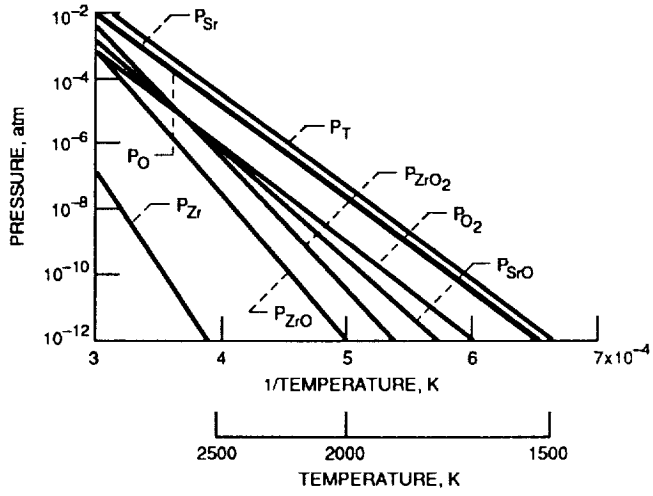

Figure 12. - Vapor pressures above $SrZrO_3$.

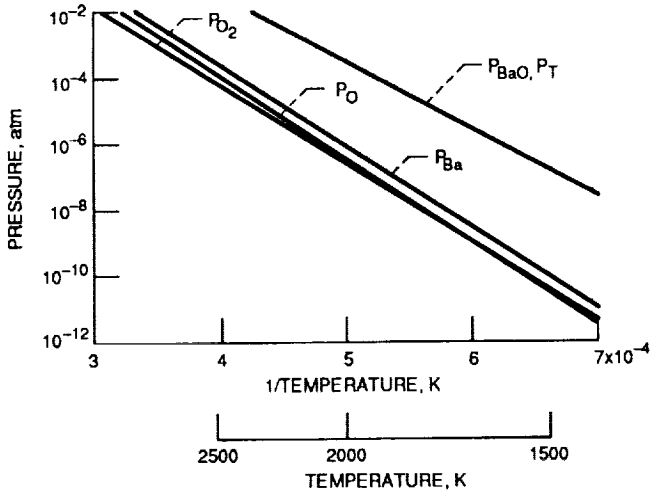

Figure 13. - Vapor pressures above BaO.

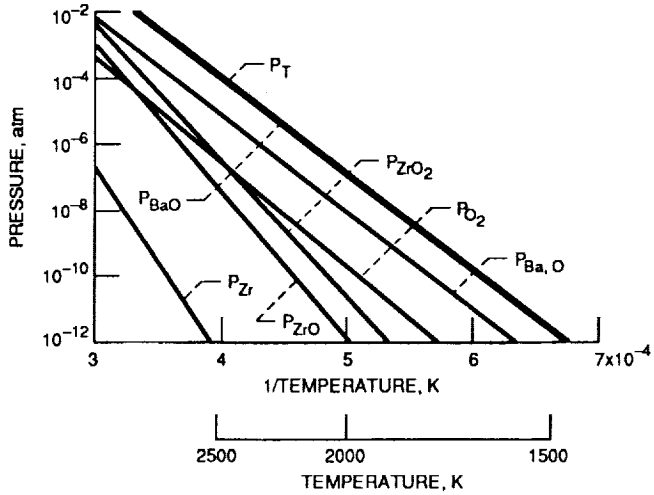

Figure 14. - Vapor pressures above $BaZrO_3$.

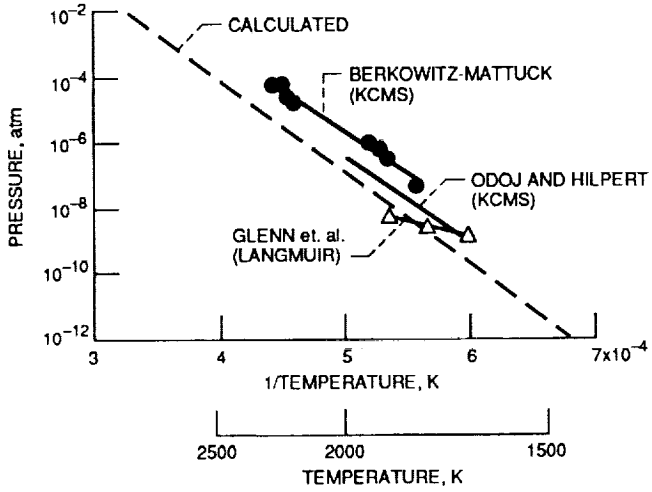

Figure 15. - Measured P(BaO) above $BaZrO_3$.

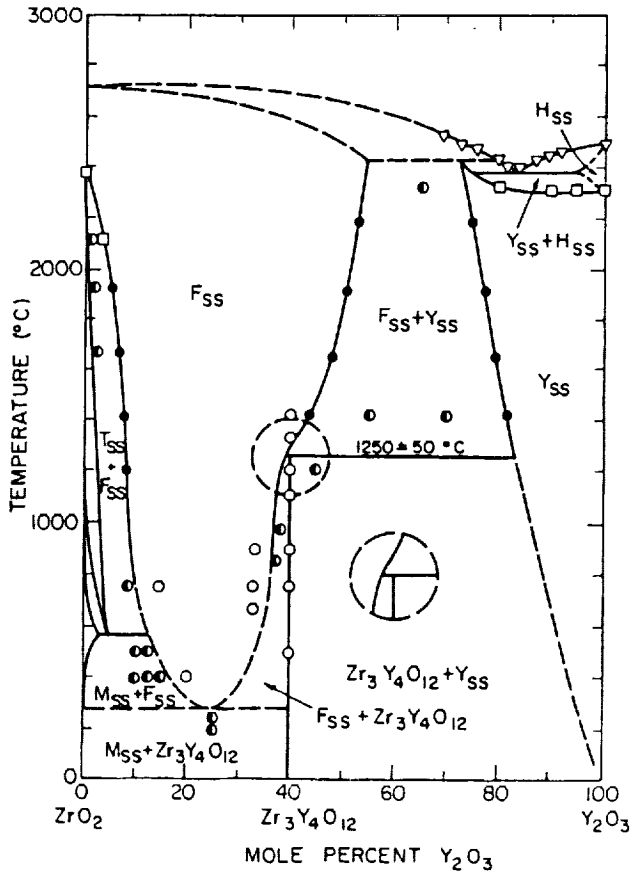

Figure 16. - Phase diagram for ZrO_2-Y_2O_3.[33] Reprinted by permission of the American Ceramic Society.

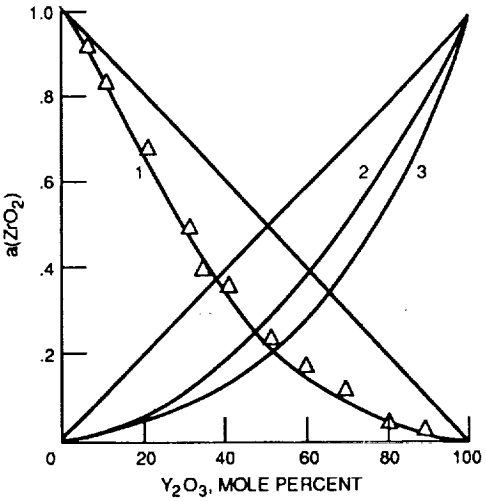

Figure 17. - Activity-composition diagram for ZrO_2-Y_2O_3.[30] Reprinted by permission of the British Library. Line 1 shows the experimental data for $a(ZrO_2)$. Line 2 shows the $a(Y_2O_3)$ values from the Gibbs-Duhem integration. Line 3 shows the $a(Y_2O_3)$obtained by comparing the values for the solid solution to the pure compound and applying the appropriate equilibrium equation.

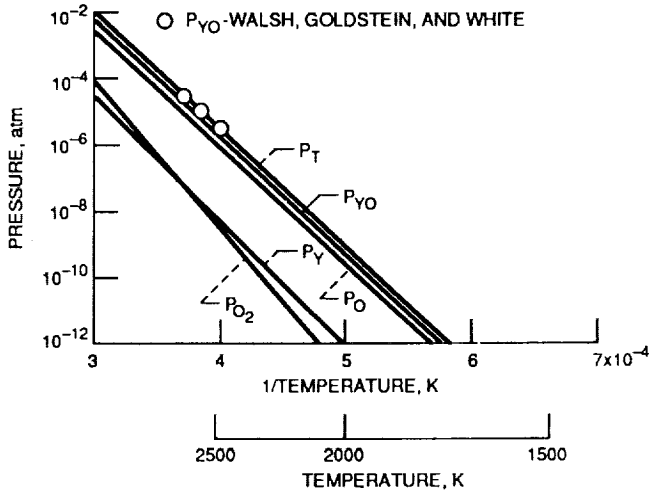

Figure 18. - Vapor pressures above Y_2O_3. Calculated and data of Walsh et. al.[34]

Sc_2O_3–ZrO_2

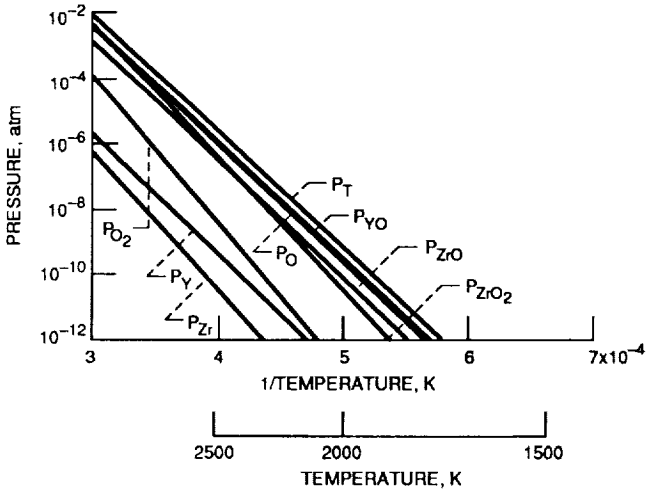

Figure 19. - Vapor pressures above $Y_2O_3 \cdot 2(ZrO_2)$.

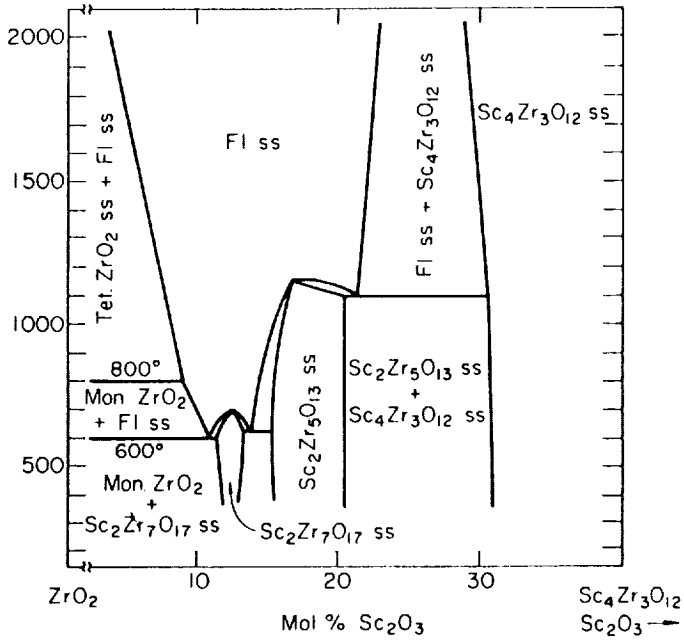

Figure 20. - Phase diagram for ZrO_2-Sc_2O_3.[36] Reprinted by permission of the American Ceramic Society.

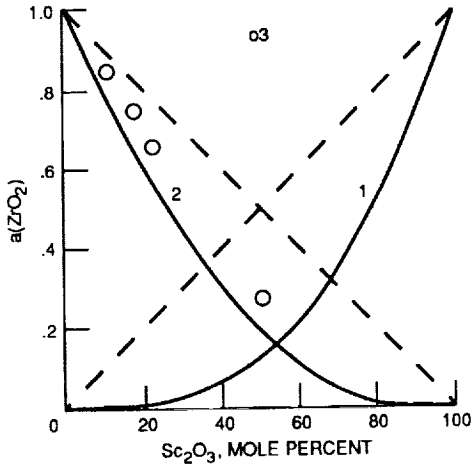

Figure 21. - Activity-composition diagram for ZrO_2-Sc_2O_3.[38] Reprinted by permission of the British Library. Lines 1 and 2 were calculated by the approximation method[32]. Point 3 is $a(ZrO_2)$ measured by comparing the solid solution to the pure compound.

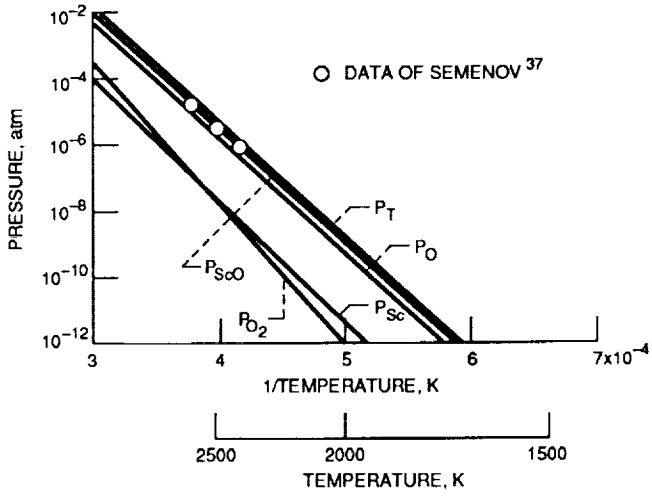

Figure 22. - Vapor pressures above Sc_2O_3.

La_2O_3-ZrO_2

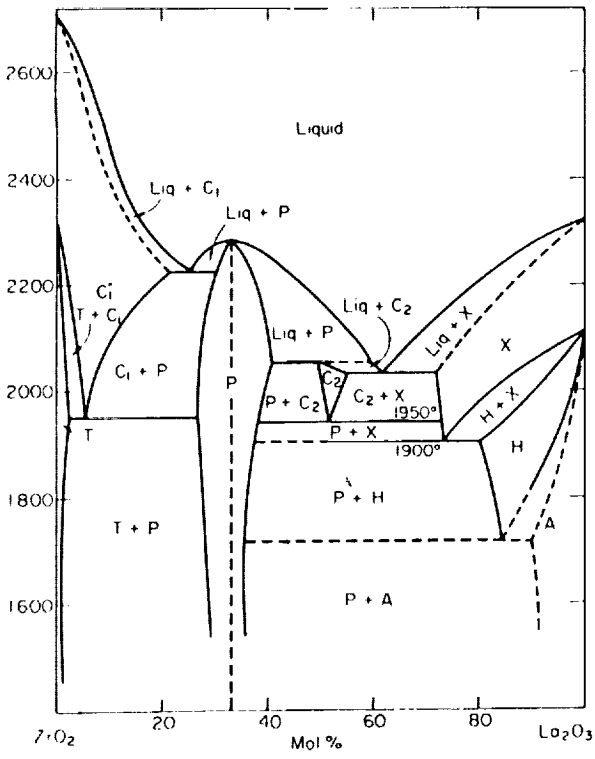

Figure 23. - Phase diagram for ZrO_2-La_2O_3.[40] Reprinted by permission of the American Ceramic Society.

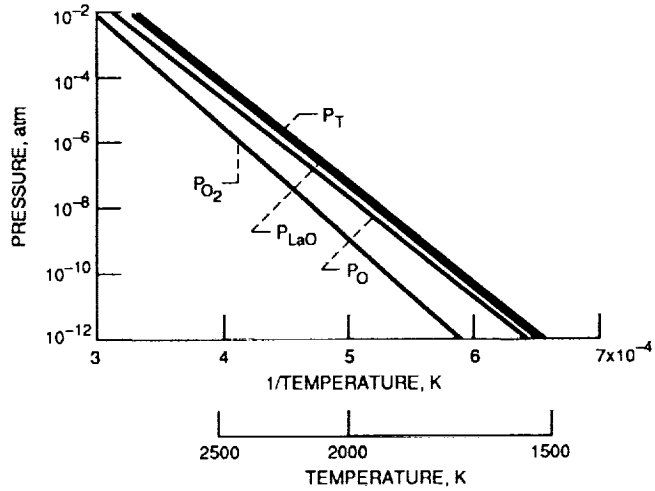

Figure 24. - Vapor pressures above La_2O_3.

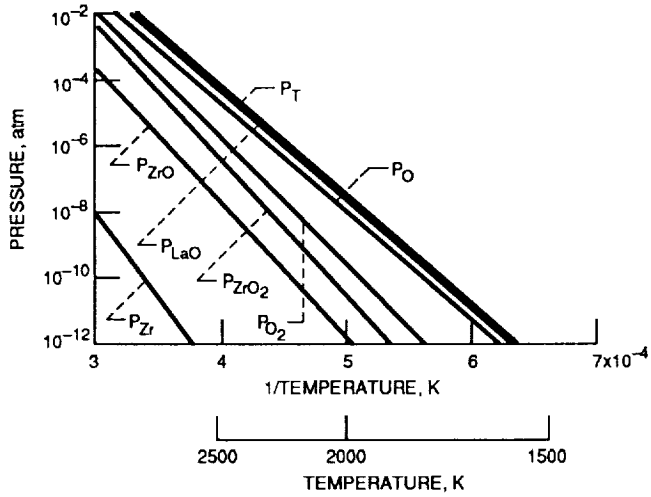

Figure 25. - Vapor pressures above $La_2O_3 \cdot 2(ZrO_2)$.

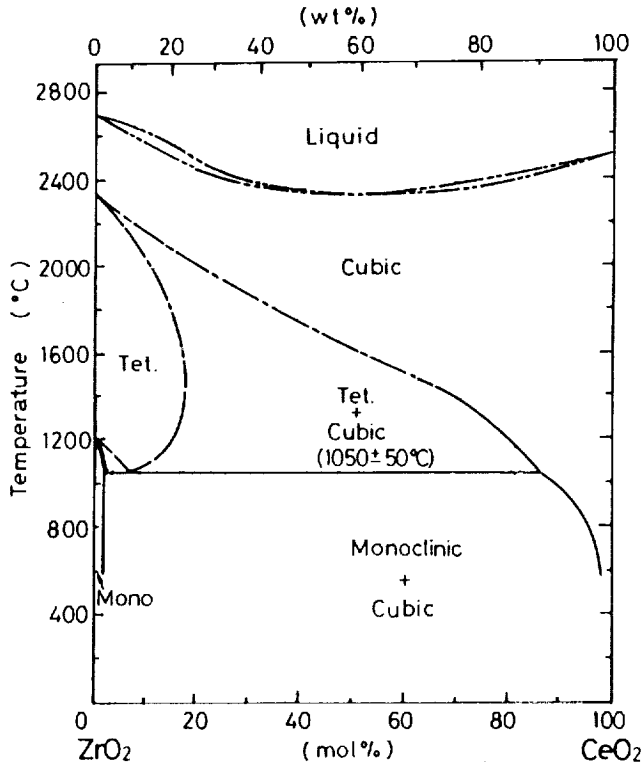

Figure 26. - Phase diagram for ZrO_2-CeO_2.[2,41] Reprinted by permission of the American Ceramic Society.

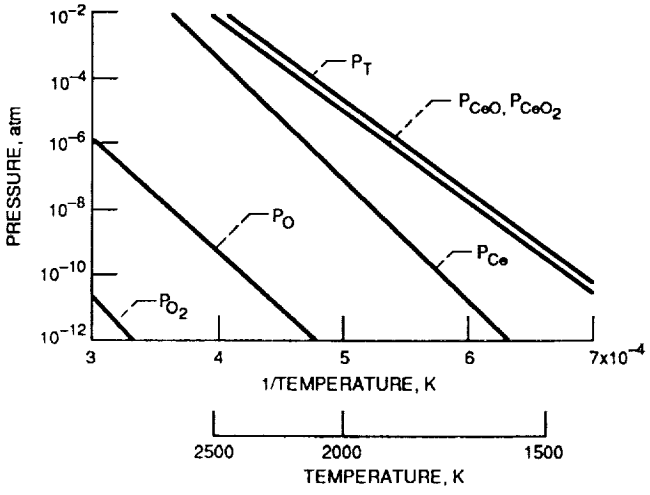

Figure 27. - Vapor pressures above Ce_2O_3.

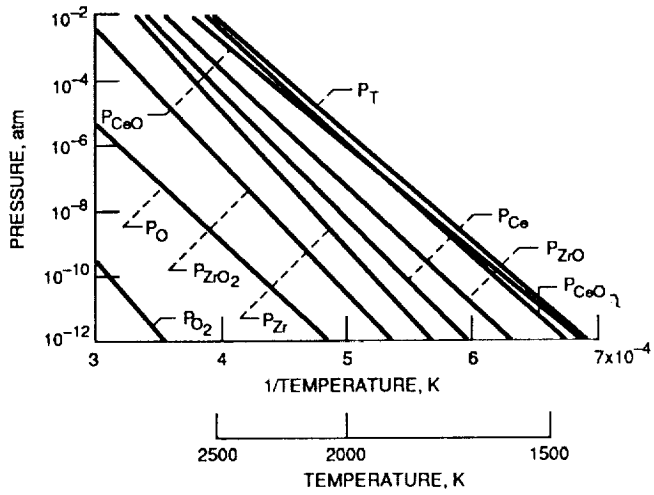

Figure 28. - Vapor pressures above $Ce_2O_3 \cdot 2(ZrO_2)$.

Sm_2O_3–ZrO_2

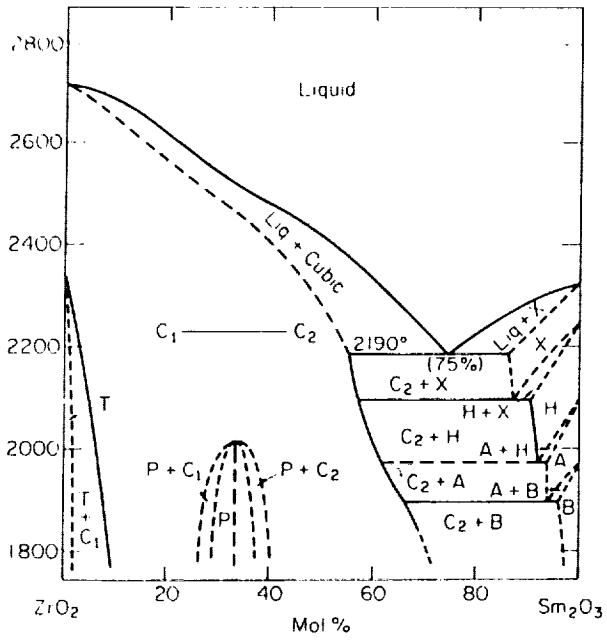

Figure 29. - Phase diagram for ZrO_2-Sm_2O_3.[42] Reprinted by permission of the American Ceramic Society.

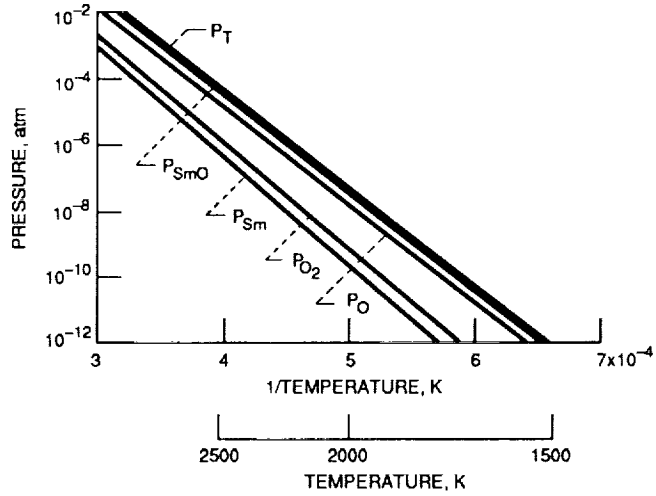

Figure 30. - Vapor pressures above Sm_2O_3.

Gd_2O_3–ZrO_2

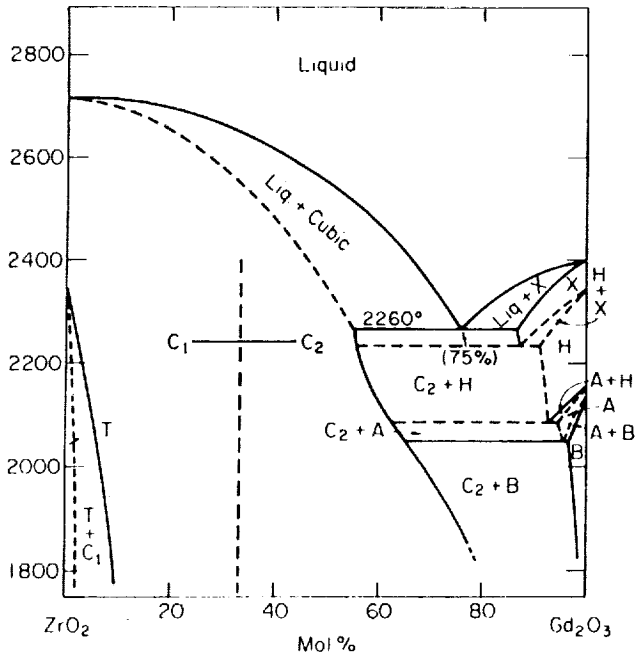

Figure 31. - Phase diagram for ZrO_2-Gd_2O_3.[44] Reprinted by permission of the American Ceramic Society.

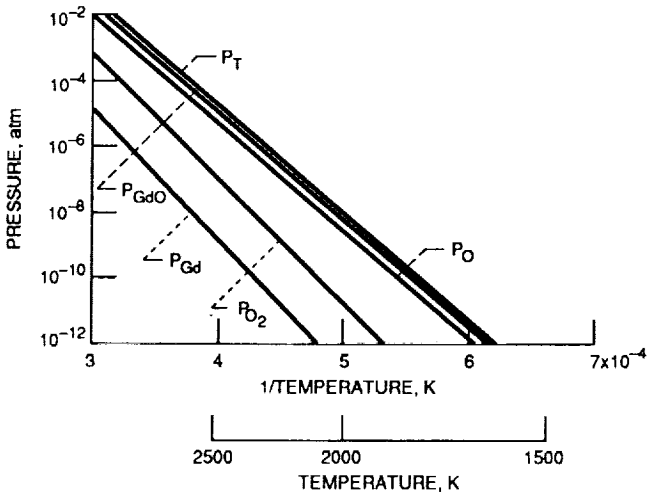

Figure 32. - Vapor pressures above Gd_2O_3.

Yb_2O_3-ZrO_2

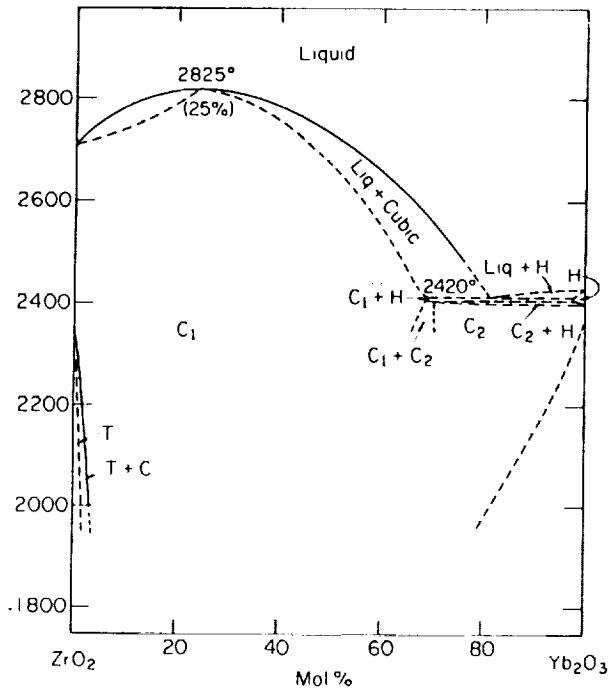

Figure 33. - Phase diagram for ZrO_2-Yb_2O_3.[45] Reprinted by permission of the American Ceramic Society.

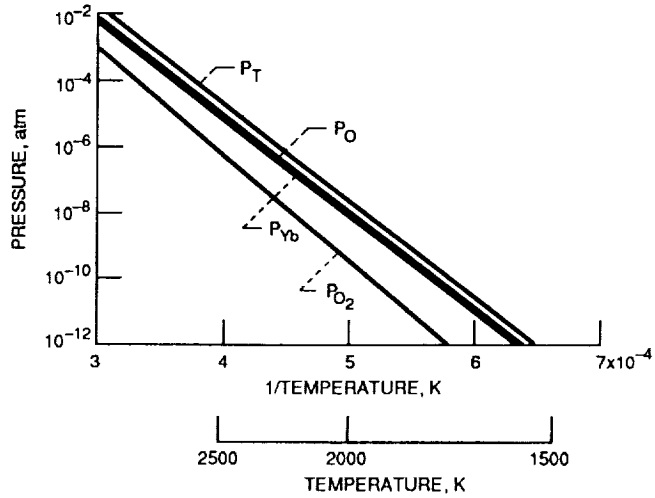

Figure 34. - Vapor pressures above Yb_2O_3.

Dy_2O_3-ZrO_2

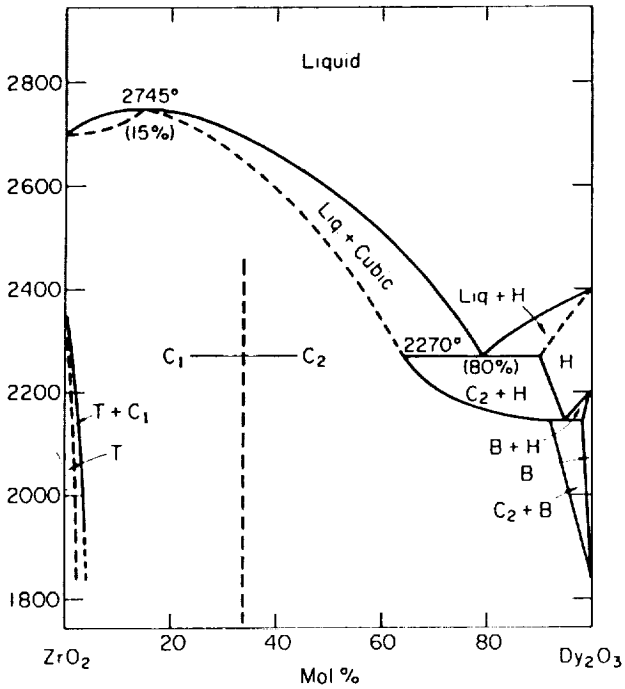

Figure 35. - Phase diagram for ZrO_2-Dy_2O_3.[46] Reprinted by permission of the American Ceramic Society.

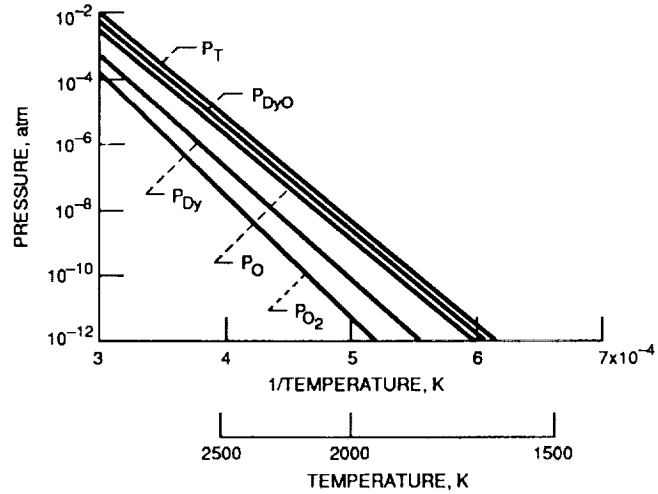

Figure 36. - Vapor pressures above Dy_2O_3.

Ho_2O_3-ZrO_2

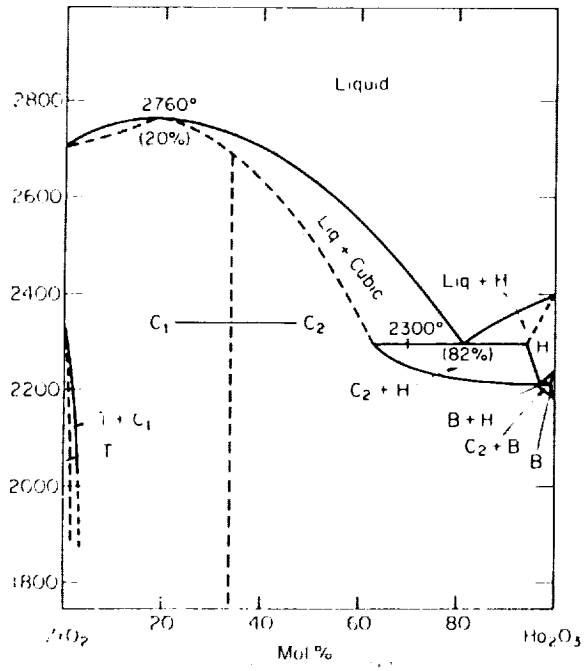

Figure 37. - ZrO_2-Ho_2O_3 phase diagram.[47] Reprinted by permission of the American Ceramic Society.

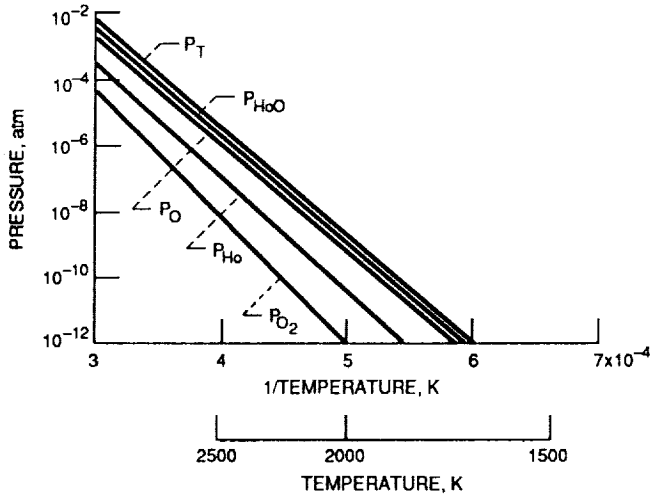

Figure 38. - Vapor pressures above Ho_2O_3.

Er_2O_3-ZrO_2

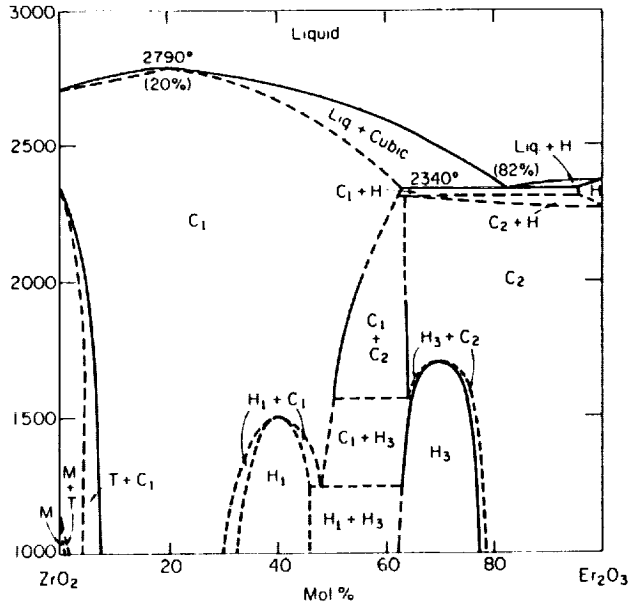

Figure 39. - ZrO_2-Er_2O_3 phase diagram.[48] Reprinted by permission of the American Ceramic Society.

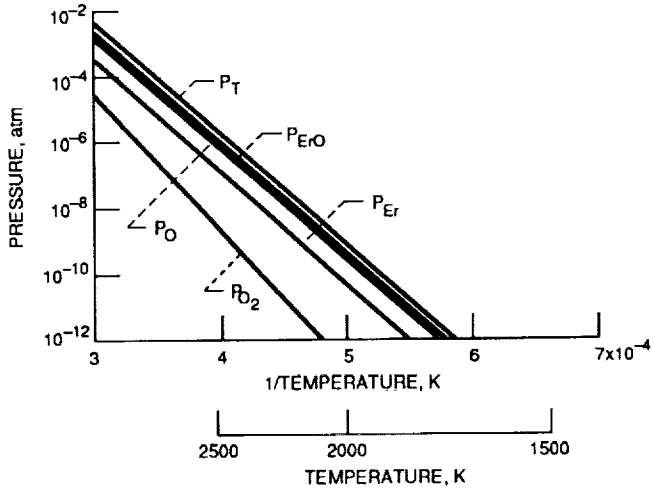

Figure 40. - Vapor pressures above Er_2O_3.

APPENDIX. THERMODYNAMIC DATA

Thermodynamic data for the more common oxides is quite plentiful; for the less common oxides it is sparse. Where possible, the best thermodynamic data was used. The most desirable information for each system is the $\Delta H_f(298)$, S(298), heat capacity and heat of any phase changes. This data is listed in Table AI.

The data for the zirconium-oxygen and alkaline earth metal-oxygen systems was taken from the JANAF tables.[1] Heat capacities were fitted to an equation of the form:

$$C_p = A + B \times 10^{-3}T + C \times 10^{5}/T^2 + D \times 10^{-6}T^2 \qquad (1)$$

The data for the alkaline earth zirconate systems were taken from other sources and is listed in Table AII. This includes both estimated and measured data. Where possible measured data were used in the final calculations, as shown in Table AI. As mentioned in the text, the $CaO\text{-}ZrO_2$ system forms a solid solution. The electrochemical data[17,18] is for the reaction of the saturated solid solution with CaO to form $CaZrO_3$. For this reason the electrochemical data cannot be directly compared to the calorimetric data. However in the case of $SrZrO_3$ and $BaZrO_3$, the two types of measurements can

be directly compared and show good agreement, as indicated in the Table AII.

Thermodynamic data for the rare earth-oxygen systems was more difficult to locate. Most of the data for the rare earth metals and condensed phase oxides was taken from the tables by Pankratz.[9] Most of these oxides vaporize to the monoxide. Data for some of the rare earth monoxides of Y and Sc was taken from the tables of Ruzinov.[10] Data for the volatile oxides of the other rare earth monoxide was available as the free energy of formation from the original sources.[14,16] The heats of formation of the solid oxide solutions of the composition $M_2O_3 \cdot 2(ZrO_2)$ were taken from the calorimetric data of Korneev et. al.[11] Entropies were estimated to be 47.8 cal/mole-^oK, after Barin and Knacke[13] and heat capacities were estimated by summing the contribution from M_2O_3 and $2(ZrO_2)$[20].

For each of the systems, the data was combined to obtain free energy of formation from the elements in their standard states. The free energy was obtained in the following form:

$$G = AG/T + BG + CG*T + DG*T^{-2} + EG*T^3 + FG*T*LOG(T) \quad (2)$$

This free energy was then put into the SOLGASMIX-PV computer program to calculate the vapor pressures for each system.

APPENDIX. REFERENCES

1. Chase, M.W., Jr., et. al., eds.: JANAF Thermochemical Tables. Third ed., American Chemical Society and American Physical Society, New York, NY, 1985.

2. Brown, R.R.; and Benington, K.O.: Thermodynamic Properties of Calcium Zirconate ($CaZrO_3$). Thermochemica Acta, vol. 106, Sept. 1986, pp. 183-190.

3. Parker, V.B.; Wagman, D.D.; and Evans, W.H.: Selected Values of Chemical Thermodynamic Properties: Tables for the Alkaline Earth Elements. NBS-TN-270-6, US Dept. of Commerce, Washington, DC, 1971.

4. Gvelesiani, G.G.; et. al.: High Temperature Enthalpy and Heat Capacity of Calcium Zirconate. Inorg. Mater. (Engl. Transl.) vol. 18, no. 6, June 1982, pp. 883-887.

5. Mezaki, R., et. al.: High-Temperature Heat Content and Thermodynamic Functions for Refractory Compounds. Advances in Thermophysical Properties at Extreme Temperatures and Pressures, S. Gratch, ed., ASME, New York, NY, 1965, pp. 138-145.

6. L'vova, A.S.; and Feodos'ev, N.N.: Heats of Formation of the Metazirconates of Calcium, Strontium, and Barium. Russ. J. Phys. Chem., vol. 38, no. 1, Jan. 1964, pp. 14-16.

7. King, E.G.; and Weller, W.W.: Low-Temperature Heat Capacities and Entropies at 298.15°K of the Zirconates of Calcium, Strontium, and Barium. US Dept. of the Interior, Bureau of Mines, BM-RI-5571, 1960.

8. Levitskii, V.A.,; Tsagareishvilli, D.Sh.; and Gvelesiani, G.G.: Enthalpy and Specific Heat of Strontium and Barium Zirconates at High Temperatures. High Temp. (Engl. Transl.), vol. 14, no. 1, Jan.-Feb. 1976, pp. 69-72.

9. Pankratz, L.B.; and Mrazek, R.V.: Thermodynamic Properties of Elements and Oxides. US Dept. of the Interior, Bureau of Mines, BU-B-672, 1983.

10. Ruzinov, L.P.; and Gulyanitski, B.S.: Equilibrium Transformations of Metallurgical Reactions (Ravnovesnye Prevrashcheniya Metallurgicheskikh Reaktsii). Metallurgiya, Moscow, 1975.

11. Korneev, V.R.; Glushkova, V.B.; and Keler, E.K.: Heats of Formation of Rare Earth Zirconates. Inorg. Mater. (Engl. Transl.), vol. 7, no. 5, May 1971, pp. 781-782.

12. Barin, I.; and Knacke, O.: Thermochemical Properties of Inorganic Substances. Springer-Verlag, 1973.

13. Barin, I.; Knacke, O. and Kubaschewski, O.: Thermochemical Properties of Inorganic Substances (Supplement)". Springer-Verlag, 1977.

14. Ackermann, R.J.; and Rauh, E.G.: A High-Temperature Study of the Stoichiometry, Phase Behavior, Vaporization Characteristics, and Thermodynamic Properties of the Cerium + Oxygen System. J. Chem. Thermodynamics, vol. 3, no. 5, Sept. 1971, pp. 609-624.

15. Kubachewski, O.: The Thermodynamic Properties of Double Oxides (A Review)", High Temp. - High Press., vol. 4, fo. 1, 1972, pp. 1-12.

16. Ames, L.L.; Walsh, P.N.; and White, D.: Rare Earths. IV. Dissociation Energies of the Gaseous Monoxides of the Rare Earths. J. Phys. Chem., vol. 71, no. 8, July 1967, pp. 2707-2718.

17. Levitskii, V.A.: Thermodynamics of Double Oxides. I. Some Aspects of the Use of CaF_2-Type Electrolyte for Thermodynamic Study of Compounds Based on Oxides of Alkaline Earth Metals. J. Solid State Chem., vol. 25, no. 1, May 1978, p. 9-22.

18. Pizzini, S. and Morlotti, R.: E.M.F. Measurements with Solid Electrolyte Galvanic Cells on the Calcium Oxide+Zirconia System. J. Chem. Soc. Faraday Trans. I, vol. 68, 1972, pp. 1601-1610.

19. Levitski, V.A., et. al.: Thermodynamic Study of Some Solid Solutions in the $CaO-ZrO_2$ System by the emf Method. J. Solid State Chem., vol. 20, no. 2, Feb. 1977, pp.119-125.

20. R.A. Swalin: Thermodynamics of Solids. Second Edition, John Wiley & Sons, New York, NY, 1962, p. 83.

TABLE A-I.

ZrO_2

Compound	ΔH_f (298), kcal/mol	S (298), cal/K mol	C_p				Temperatures		Comments	Source
			A	B	C	D				
Zr(α)	0	9.290	6.016	−0.106	−0.124	1.320	298	1135		1
Zr(β)			7.783	−2.334	−.153	1.280	1135	2125	Δ(α–β) = 0.960	
Zr(L)			10.000						Δ(β–L) = 5.000	
Zr(g)	145.8	43.745	4.522	1.637	0.896	−0.129	298	2500		1
ZrO_2(α)	−262.3	12.036	16.64	1.80	−3.36		298	1478		1
ZrO_2(β)			17.80				1478	2950	Δ(α–β) = 1.42	
ZrO_2(L)			20.8				2950	3300	Δ(β–L) = 20.8	
ZrO_2(g)	−68.400	65.402	12.601	1.288	−1.783	−0.328	298	2400		1
ZrO(g)	14.0	54.33	6.28	3.56			298	2000		1
ZrO(g)			14.120	−.839			2000	2500		1
O(g)	59.554	38.494	5.019	−0.055	0.208	1.587×10^{2}	298	2500		1
O_2(g)	0	49.031	6.922	1.676	−0.362	−0.300	298	2500		1

MgO

Compound	ΔH_f (298), kcal/mol	S (298), cal/K mol	C_p				Temperatures		Comments	Source
			A	B	C	D				
Mg(S)	0	7.809	6.252	−0.209	−0.375	1.983	298	923		1
Mg(L)			8.200				923	2000	Δ(S–L) = 2.026	
Mg(g)	35.158	35.528	4.968				298	1700		1
Mg(g)			5.347	−0.286	−1.936	6.056×10^{-2}	1700	2700		
Mg_2(g)	68.744	57.406	4.986	-3.714×10^{-2}	0.738	1.800×10^{-2}	298	1700		1
Mg_2(g)			20.338	−11.490	−81.813	2.431	1700	2500		
MgO(S)	−143.700	6.435	11.360	1.215	−2.540	−0.103	298	2500		1
MgO(g)	13.900	50.973	−4.093	31.071	3.402	−14.188	298	1000		1
			26.184	−11.980	−34.208	2.331	1000	2400		

TABLE A-I. - Continued.

CaO

Compound	ΔH_f (298), kcal/mol	S (298), cal/K mol	C_p				Temperatures		Comments	Source
			A	B	C	D				
Ca(α)	0	9.940	3.925	5.241	0.630	4.685×10^{-2}	298	716		1
Ca(β)			1.307	8.035	2.734	-.124	716	1115	Δ(α-β) = 0.222	
Ca(L)							1115	2500	Δ(β-L) = 2.041	
Ca(g)	42.495	37.019	4.968				300	1200		1
			7.708	-2.374	-10.675	0.579	1200	2500		
CaO(S)	-151.790	9.133	11.978	1.088	-1.988	-3.156×10^{-2}	300	2500		1
CaO(g)	10.500	52.514	9.884	-2.648	-1.338	1.737	300	2500		1
$CaZrO_3$(S)	-422.3	23.9	30.15	1.54	-6.05		298	2000		2,4,7

SrO

Compound	ΔH_f (298), kcal/mol	S (298), cal/K mol	C_p				Temperatures		Comments	Source
			A	B	C	D				
Sr(α)	0	13.311	5.634	2.424	3.590×10^{-2}	7.881×10^{-2}	300	820		1
Sr(β)							820	1050	Δ(α-β) = 0.200	
Sr(L)							1050	2000	Δ(β-L) = 1.776	
Sr(g)	39.197	39.293	4.968				298	1300		1
			8.952	-3.459	-15.517	0.846	1300	2500		
SrO(S)	-141.500	13.270	11.665	1.934	-1.235	-0.094	298	2500		1
SrO(g)	-3.200	54.985	10.282	-3.134	-1.446	1.830	298	2500		1
$SrZrO_3$(S)	-425.2	27.5	29.79	1.40	-4.89		298	1620		3,7,8

TABLE A-I. - Continued.

BaO

Compound	ΔH_f (298), kcal/mol	S (298), cal/K mol	C_p				Temperatures		Comments	Source
			A	B	C	D				
Ba(α)	0	14.932	9.584	-24.742	-0.183	52.831	100	583		1
Ba(β)			-1.059	14.402	-2.181	3.158	583	768	Δ(α-β) = 0	
Ba(γ)			9.337				768	1000	Δ(β-γ) = 0	
Ba(L)			15.979	-8.183	.901	2.464	1000	2100	Δ(β-L) = 1.915	
Ba(g)	42.800	40.690	4.968				300	900		1
			8.196	-5.379	-2.247	2.360	900	2500		
BaO(S)	-131.00	17.225	11.809	2.076	-1.002	-0.142	298	2200		1
BaO(g)	-29.60	56.28	8.979	-0.223	-0.965	0.156	298	2500		1
$BaZrO_3$(α)	-426.73	29.8	25.63	6.24	-2.82		298	758		3,7,8
$BaZrO_3$(β)			27.77	-.18			758	1175		
$BaZrO_3$(γ)			24.75	4.42			1175	1606	Δ(β-γ) = 0.33	

Y-O

Compound	ΔH_f (298), kcal/mol	S (298), cal/K mol	C_p				Temperatures		Comments	Source
			A	B	C	D				
Y(α)	0	10.620	5.718	1.810	0.073		298	1752		9
Y(β)			8.360				1752	1799	Δ(α-β) = 1.193	
Y(L)			10.300				1799	2500	Δ(β-L) = 2.724	
Y(g)	100.700	42.869	5.510	-0.178	0.644		298	2500		9
YO(g)	-9.3	55.88	8.410	0.320	-0.840		298	2000		10
Y_2O_3(α)	-455.38	23.690	29.421	1.414	-4.749		298	1330		9
Y_2O_3(β)			31.500				1330	2000	Δ(α-β) = 0.310	
$Y_2Zr_2O_7$	-985.18	47.8	62.9	4.8	-11.5		298	1500		11,13

TABLE A-I. - Continued.

Sc-O

Compound	ΔH_f (298), kcal/mol	S (298), cal/K mol	C_p				Temperatures		Comments	Source
			A	B	C	D				
Sc(α)	0	8.280	4.884	2.678	0.371		298	1608		9
Sc(β)			10.570				1608	1812	Δ(α-β) = 0.958	
Sc(L)			10.570				1812	3000	Δ(β-L) = 3.369	
Sc(g)	90.300	41.749	4.887	0.100	0.335		298	2500		9
ScO(g)	-13.680	53.500	8.220	0.440	-0.870		298	2000		10
Sc_2O_3(S)	-456.220	18.400	27.709	2.780	-5.351		298	2762		9

La-Zr-O

Compound	ΔH_f (298), kcal/mol	S (298), cal/K mol	C_p				Temperatures		Comments	Source
			A	B	C	D				
La(α)	0	6.480	6.585	0.100	-0.120		298	550		9
La(β)			4.319	3.504	.768		550	1134	Δ(α-β) = 0.087	
La(y)			9.475				1134	1193	Δ(α-y) = 0.746	
La(L)			8.200				1193	2000	Δ(y-L) = 1.481	
La(g)	103.000	43.564	6.000	1.162	-0.808		298	2000		9
LaO(g)	-26.000	58.300	8.460	0.300	-0.840		298	2000		10
La_2O_3(S)	-428.700	30.430	28.617	3.400	-3.228		298	2000		9
$La_2Zr_2O_7$(S)	-975.6	47.8	61.90	7.00	-9.95		298	1478		11
$La_2Zr_2O_7$(S)			64.22	3.40	-3.23		1478	2000		

TABLE A-I. - Continued.

Ce–Zr–O

Compound	ΔH_f (298), kcal/mol	S (298), cal/K mol	C_p				Temperatures		Comments	Source
			A	B	C	D				
Ce(γ)	0	17.200	5.085	3.894	0.172		298	999		9
Ce(δ)			8.990				999	1071	Δ(γ–δ) = 0.175	
Ce(L)			9.010				1071	2000	Δ(δ–L) = 1.305	
Ce(g)	101.000	45.807	6.169	2.154	−1.153		298	2000		9
CeO_2(S)	−260.200	14.890	16.761	2.216	−2.392		298	2000		9
Ce_2O_3(S)	−429.300	35.400	31.358	4.664	−4.142		298	1000		9
$Ce_2Zr_2O_{7+x}$(S)	−997.9	47.8	64.64	8.26	−10.86		298	1478		11
			66.96				1478	2950		
CeO(g)			ΔG = −37 360 − 10.8T				1600	2000		14
CeO_2(g)			ΔG = −131 350 + 7.0T				1600	2000		14

Sm–O

Compound	ΔH_f (298), kcal/mol	S (298), cal/K mol	C_p				Temperatures		Comments	Source
			A	B	C	D				
Sm(α)	0	16.630	8.200	2.970	−1.800		298	1190		9
Sm(β)			11.220				1190	1345	Δ(α–β) = 0.744	
Sm(L)			12.000				1345	2000	Δ(β–L) = 2.060	
Sm(g)	49.400	43.722	7.895	−0.670	−0.391		298	2000		9
Sm_2O_3(S)	−435.860	36.100	30.484	4.888	−4.064		298	1195	Monoclinic	9
			36.900				1195	2000	Δ(α–β) = 0.250	
Sm_2Zr_2O7	−978.900	47.800	63.76	8.49	−10.78		298	1195		11
			70.18	3.60	−6.72		1195	1478		
			72.50				1478	2000		
SmO(g)			ΔG = −5.953T − 47 688							16

TABLE A-I. - Continued.

Gd–O

Compound	ΔH_f (298), kcal/mol	S (298), cal/K mol	C_p				Temperatures		Comments	Source
			A	B	C	D				
Gd(α)	0	16.240	2.786	4.406	4.231		298	1533		9
Gd(β)			6.827				1533	1585	Δ(α–β) = 0.935	
Gd(L)			8.880				1585	2000	Δ(β–L) = 2.403	
Gd(g)	95.000	46.416	6.273	-0.252	-0.343		298	2000		9
Gd_2O_3(m)	-434.900	37.500	27.365	3.458	-2.588		298	2000		9
$Gd_2Zr_2O_7$	-972.000	47.8	60.65	7.06	-9.31		298	1478		
			62.97	3.46	-2.59		1478	2950		13
GdO(g)			ΔG = -11.675T + -28 781							16

Yb–O

Compound	ΔH_f (298), kcal/mol	S (298), cal/K mol	C_p				Temperatures		Comments	Source
			A	B	C	D				
Yb(S)	0	14.300	1.024	11.404	1.747		298	553		9
Yb(α)			6.228	1.388	.227		553	1033	Δ(S–α) = 0	
Yb(β)			8.640				1033	1097	Δ(α–β) = 0.418	
Yb(L)			8.786				1097	1467	Δ(β–L) = 1.830	
Yb(g)	36.350	41.352	4.968				298	2000		9
Yb_2O_3(α)	-433.680	31.800	31.817	0.062	-3.792		298	1365		9
YbO_3(β)			32.150				1365	2000	Δ(α–β) = 0.150	

TABLE A-I. - Concluded.

Dy-O

Compound	ΔH_f (298), kcal/mol	S (298), cal/K mol	C_p				Temperatures		Comments	Source
			A	B	C	D				
Dy(α)	0	17.900	3.490	4.450	1.692		298	1657		9
Dy(β)			6.700				1657	1682	Δ(α-β) = 0.995	
Dy(L)			11.930				1682	2000	Δ(β-L) = 2.643	
Dy(g)	69.400	46.794	4.444	0.726	0.274		298	2000		9
Dy_2O_3(α)	-445.320	35.800	29.826	2.774	-2.545		298	1590		9
Dy_2O_3(β)			34.400				1590	2000	Δ(α-β) = 0.220	
DyO(g)			ΔG = -6.723T - 35 621				1800	2000		16

Ho-O

Compound	ΔH_f (298), kcal/mol	S (298), cal/K mol	C_p				Temperatures		Comments	Source
			A	B	C	D				
Ho(α)	0	17.430	3.341	4.650	1.567		298	1701		9
Ho(β)			6.700				1701	1743	Δ(α-β) = 1.121	
Ho(L)			10.500				1743	2000	Δ(β-L) = 2.911	
Ho(g)	71.900	46.718	4.705	0.358	0.139		298	2000		9
Ho_2O_3(S)	-449.550	37.800	30.364	1.332	-2.917		298	2000		9
HoO(g)			ΔG = -6.333T + -35 789							16

Er-O

Compound	ΔH_f (298), kcal/mol	S (298), cal/K mol	C_p				Temperatures		Comments	Source
			A	B	C	D				
Er(S)	0	17.490	5.280	2.518	0.603		298	1795		9
Er(L)			9.250				1795	2000	Δ(S-L) = 4.757	
Er(g)	75.800	46.347	4.114	1.046	0.482		298	2000		9
Er_2O_3(S)	-453.590	37.200	28.864	2.542	-3.282		298	2000		9
ErO(g)			ΔG = -7.090T + -29 596				1800	2000		16

TABLE A-II.

Thermodynamic Data for $CaZrO_3$

Reference	ΔH_f (298), kcal/mol	S (298), cal/K mol	C_p	Comments
Brown and Bennington (2)	-424.58±0.47			HF solution calorimetry
L'vova and Feodose'v (6)	-418.7			Bomb calorimetry
Parker (3)	-422.3	23.92		Value of L'vova and Feodose'v corrected with recent $\Delta H_f(ZrO_2)$
Kubachewski (15)		22.4		Estimated
King and Weller (7)		23.9±0.2		Calorimetry
Gvelesiani et al. (4)			$30.15 + 1.54\times10^{-3}T - 6.05\times10^{5}/T^2$	Calorimetry
Mezaki et al. (5)			$30.41 + 5.19\times10^{-3}T - 3.46\times10^{5}/T^2$	Calorimetry
Barin and Knacke (12)	-421.9	22.4	$28.5 + 2.88\times10^{-3}T - 5.02\times10^{5}/T^2$	

Thermodynamic Data for $SrZrO_3$

Reference	ΔH_f (298), kcal/mol	S (298), cal/K mol	C_p	Comments
L'vova and Feodose'v (6)	-418.3			Bomb calorimetry
Parker (3)	-422.4	27.5		See $CaZrO_3$-Parker comment
Levitskii et al. (8)			$29.79 + 1.4\times10^{-3}T - 4.89\times10^{5}/T^2$	
King and Weller (7)		27.5±0.2		Calorimetry
Levitskii (17)	-425.2			Electrochemical cell
Barin and Knacke (12)	-425.0	26.0	$28.98 + 2.92\times10^{-3}T - 5.166\times10^{5}/T^2$	
Kubachewski (15)	-418.3	26.0±2.0		S-estimated

TABLE A-II. -Concluded.

Thermodynamic Data for $BaZrO_3$

Reference	ΔH_f (298), kcal/mol	S (298), cal/K mol	C_p	Comments
L'vova and Feodose'v (6)	-421.1			Bomb calorimetry
Parker (3)	-425.3	29.8		See $CaZrO_3$-Parker comment
Levitskii et al. (8)			α 25.63 + $6.24\times10^{-3}T$ - $2.82\times10^{5}/T^2$ β 27.77 - $0.18\times10^{-3}T$ γ 24.75 + $4.42\times10^{-3}T$	
King and Weller (7)		29.8±0.3		
Levitskii (17)	-426.73±0.58			Electrochemical cell
Barin and Knacke (12)	-423.2	26.5	29.35 + $2.1\times10^{-3}T$ - $5.25\times10^{5}/T^2$	
Kubachewski (15)		26.5±2.0		

NASA
National Aeronautics and Space Administration

Report Documentation Page

1. Report No.	2. Government Accession No.	3. Recipient's Catalog No.
NASA TM-102351		

4. Title and Subtitle	5. Report Date
Thermodynamic Properties of Some Metal Oxide-Zirconia Systems	December 1989
	6. Performing Organization Code

7. Author(s)	8. Performing Organization Report No.
Nathan S. Jacobson	E-5060
	10. Work Unit No.
	510-01-01

9. Performing Organization Name and Address	11. Contract or Grant No.
National Aeronautics and Space Administration Lewis Research Center Cleveland, Ohio 44135-3191	
	13. Type of Report and Period Covered
	Technical Memorandum

12. Sponsoring Agency Name and Address	14. Sponsoring Agency Code
National Aeronautics and Space Administration Washington, D.C. 20546-0001	

15. Supplementary Notes

16. Abstract

Metal oxide-zirconia systems are a potential class of materials for use as structural materials at temperatures above 1900 K. These materials must have no destructive phase changes and low vapor pressures. Both alkaline earth oxide (MgO, CaO, SrO, and BaO)-zirconia and some rare earth oxide (Y_2O_3, Sc_2O_3, La_2O_3, CeO_2, Sm_2O_3, Gd_2O_3, Yb_2O_3, Dy_2O_3, Ho_2O_3, and Er_2O_3)-zirconia system are examined. For each system, the phase diagram is discussed and the vapor pressure for each vapor specie is calculated via a free energy minimization procedure. The available thermodynamic literature on each system is also surveyed. Some of the systems look promising for high temperature structural materials.

17. Key Words (Suggested by Author(s))	18. Distribution Statement
Zirconia Oxides Vapor pressures High temperature materials	Unclassified – Unlimited Subject Category 27

19. Security Classif. (of this report)	20. Security Classif. (of this page)	21. No of pages	22. Price*
Unclassified	Unclassified	62	A04

*For sale by the National Technical Information Service, Springfield, Virginia 22161